USDRIVE

DRIVING RESEARCH AND INNOVATION FOR VEHICLE EFFICIENCY AND ENERGY SUSTAINABILITY

U.S. DRIVE Highlights of Technical Accomplishments 2020

April 2021

U.S. DRIVE
Highlights of Technical Accomplishments Overview

Through precompetitive collaboration and technical exchange, U.S. DRIVE accelerates the development of energy-efficient advanced automotive and energy infrastructure technologies.

U.S. DRIVE (*Driving Research for Vehicle efficiency and Energy sustainability*) is a voluntary government-industry partnership focused on precompetitive, advanced automotive and related infrastructure technology research and development. Partners are the United States Department of Energy (DOE) and leaders in the automotive industry (United States Council for Automotive Research LLC, the collaborative technology company of FCA US LLC, Ford Motor Company, and General Motors); energy industry (BP, Chevron, Phillips 66, ExxonMobil, and Shell); and electric utility industry (American Electric Power, DTE Energy, Duke Energy, Southern California Edison, and the Electric Power Research Institute).

The Partnership benefits from a history of successful collaboration across multiple technical areas, each focused on a key area of the U.S. DRIVE portfolio (see below). These teams convene the best and brightest scientists and engineers from across the Partnership to discuss key technical challenges, identify possible solutions, and evaluate progress toward goals and targets published in technology roadmaps. By providing a framework for frequent and regular interaction among technical experts in common areas of expertise, U.S. DRIVE accelerates technical progress, helps to avoid duplication of efforts, ensures that publicly-funded research delivers high-value results, and overcomes high-risk barriers to technology commercialization.

U.S. DRIVE teams selected the highlights in this document from many hundreds of DOE-funded projects conducted by some of the nation's top research organizations. Each one-page summary represents what Partnership experts collectively consider to be significant progress in the development of advanced automotive and infrastructure technologies. The report features technical highlights in two general categories:

Vehicles

- Advanced Combustion and Emission Control
- Electrical and Electronics
- Electrochemical Energy Storage
- Fuel Cells
- Materials

Infrastructure and Integration

- Grid Integration
- Hydrogen Codes and Standards
- Hydrogen Delivery and Storage
- Hydrogen Production
- Net-Zero Carbon Fuels
- Vehicle and Mobility Systems Analysis

More information about U.S. DRIVE, including prior-year accomplishments reports and technology roadmaps, is available on the DOE (https://www.energy.gov/eere/vehicles/us-drive) and USCAR (www.uscar.org) web sites.

Contents

VEHICLES

Advanced Combustion and Emission Control

2020 U.S. DRIVE Highlight

Direct Numerical Simulation of Flow and Heat Transfer in Internal Combustion Engines

The data generated from these simulations can lead to significantly improved understanding of in-cylinder processes and accurate models for engineering simulations.

Argonne National Laboratory

Comprehensive understanding of intake airflows and fuel sprays over a wide operating range through advanced high-fidelity modeling tools has been identified as a bottleneck to increased adoption of advanced dilute combustion gasoline engines. Engine manufacturers currently use commercial codes that have inherent limitations in predictive capability and to massive parallelization. With the emergence of highly scalable, high-order simulation tools developed using investments from the U.S. Department of Energy's exascale computing project and the availability of leadership class supercomputers, high-fidelity numerical simulations have emerged as a viable asset in improving our understanding of the multiscale/multi-physics in-cylinder processes and the impact of design changes on internal combustion engine (ICE) performance.

Researchers from the Energy Systems (ES) and Computational Sciences (CPS) divisions at Argonne National Laboratory recently performed the first ever Direct Numerical Simulations (DNS) of the compression and expansion strokes of the GM TCC-III engine at motored operating conditions. These simulations, performed with the open-source Nek5000 code using more than 400 million gridpoints on more than 50,000 processors of Argonne's Theta supercomputer, have delivered unprecedented insights into the turbulent flow-field and near-wall heat transfer characteristics in an ICE. The DNS calculation was initialized using the velocity and temperature fields from a precursor multi-cycle wall-resolved large eddy simulation calculation. Accuracy of several traditional wall function models to predict the near-wall heat flux was analyzed across a range of crank angles and it was shown that all the models underpredicted the heat flux by as much as 50% (Fig. 1). The DNS dataset is currently being used to develop improved wall heat transfer models. Simulations are also being planned on more modern engine platforms such as Sandia's direct injection spark ignition and upcoming Partnership to Advance Combustion Engines consortium engines and will complement engine experiments.

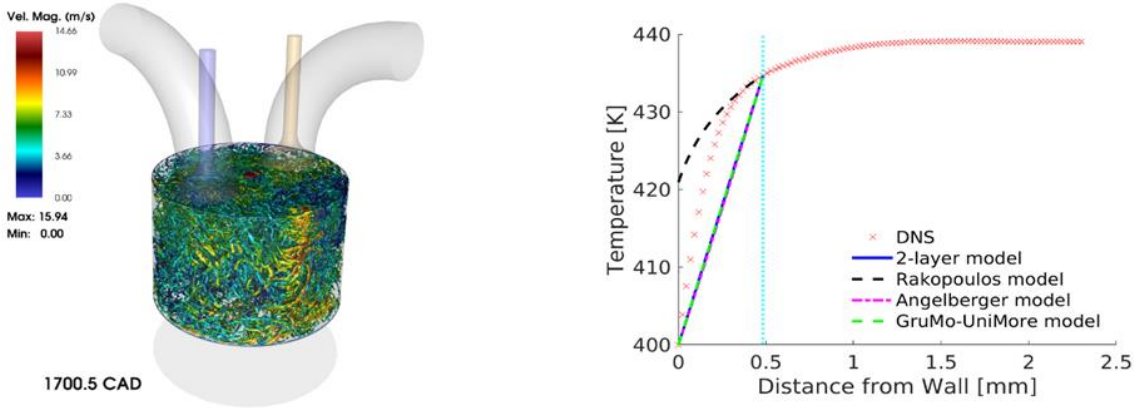

Figure 1. Left: Snapshot of turbulent eddies during the compression stroke from the DNS calculation. Right: Comparison of the near-wall temperature field predicted by DNS compared to the predictions by different commonly used wall function models.

2020 U.S. DRIVE Highlight

Machine Learning Tool and Model Link Injector Wear with Reduced Performance

Experimentally validated simulation toolkit predicts locations of cavitation and erosion in multi-hole injectors, aided by new deep learning approach.

Argonne National Laboratory

To comply with regulation standards, direct injection engines have steadily increased injection pressure. However, these conditions can lead to erosion in fuel injectors and reduce performance. Manufacturers must certify engine emissions for their full useful lives, and the need to minimize injector wear can often preclude running under the most efficient operating conditions. To develop accurate models for injector durability, researchers at Argonne National Laboratory carried out a joint experimental and computational study of the impact of erosion on injector performance.

In-situ X-ray imaging was used to study cavitation erosion within the injector. The multi-hole injector tips were fabricated from aluminum to accelerate the erosion process. Using CTSegNet, a new software toolkit for X-ray image processing, high-resolution X-ray scans were processed into a three-dimensional geometry and revealed unique erosion patterns in the orifices (Fig.1). CTSegNet speeds the processing of tomography data from raw X-ray images to 3D geometries using deep learning. The tool was "trained" on manually generated data, and "learned" to process new data sets without manual intervention. Data processing that used to require weeks of work was reduced to minutes of compute time. The optimized workflow with CTSegNet has allowed more nozzles to be scanned in the past year than in the previous five years combined.

Researchers used the Cavitation-Induced Erosion Risk Assessment (CIERA) toolkit to simulate the internal flow through the baseline and eroded injector geometries. The cavitation development in the eroded injector was predicted to significantly affect performance, with an 8%-10% decrease in the injection velocity and fuel flow rate relative to the baseline geometry. CIERA has been integrated into a common engine simulation platform to predict cavitation and wear in fuel injectors, and has been employed to link injector wear with combustion and emissions. Using this toolkit, engine manufacturers can gain a clear view of the long-term performance of injectors, and optimize their engine designs for the lifetime of the vehicle.

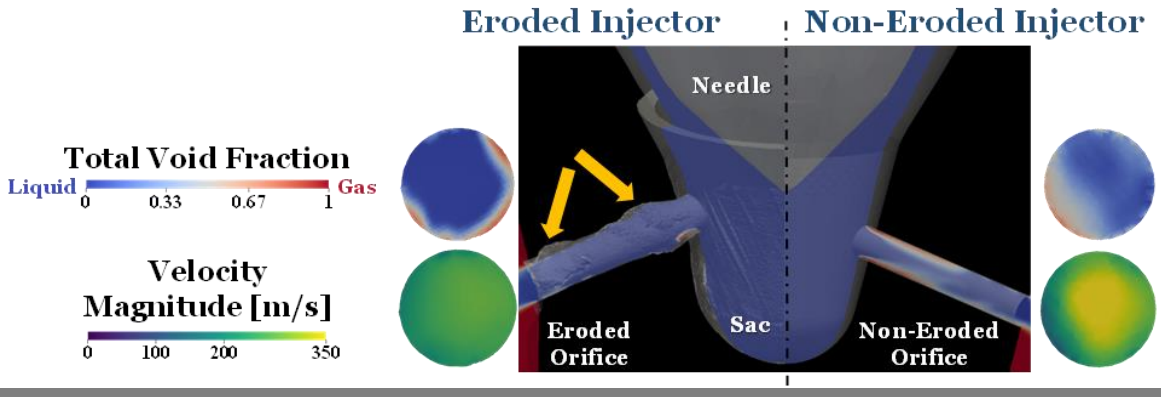

Figure 1. High resolution X-ray scans of an eroded multi-hole injector conducted at Argonne's Advanced Photon Source revealed erosion damage in the injector orifices, as indicated by the yellow arrows. Comparison of the predicted injection conditions from the eroded orifice (left) and non-eroded orifice (right) highlight the impact of erosion on cavitation formation, injection velocity, and ultimately fuel delivery rate.

2020 U.S. DRIVE Highlight

Simulations Provide New Insights into Pre-Spark Heat Release in Boosted Spark Ignition Engines

New simulation best practices capture the physics of low-temperature pre-spark heat release for internal combustion engines, paving the way to better engine knock control.

Argonne National Laboratory

Accurate capture of low-temperature heat release (LTHR) is critical for predicting auto-ignition processes in internal combustion engines (ICEs). While LTHR is typically obscured by the deflagration, extremely late ignition phasing can lead to LTHR prior to the spark, i.e., pre-spark heat release (PSHR). Argonne researchers developed new computational fluid dynamics best practices to model PSHR in a boosted direct-injection spark ignition (SI) internal combustion engine. A hybrid approach was proposed, based on the *G*-equation model for representing the turbulent flame front, and the well-stirred reactor model for tracking the chemistry in the unburnt region. Multicycle simulations were performed with Co-Optima Alkylate and E30 fuels. Different than common SI modeling practices, the well-stirred reactor model must be kept active throughout the entire simulation. At the slightly increased cost of simulation run time, the predicted in-cylinder pressure and heat release rate agreed well with experimental data provided by researchers at Oak Ridge National Laboratory (Figure 1, left). It was also noted that a RANS framework was sufficient to capture the average cycle behavior and some of the cycle-to-cycle variability observed in the experiments at Oak Ridge National Laboratory.

The dynamics of PSHR were analyzed in detail by means of the pressure-temperature trajectory framework (Figure 1, middle). Analysis showed that the occurrence of PSHR is correlated with the first-stage ignition delay of the fuel. It was also revealed that the trapped in-cylinder residuals have a strong impact on the onset of PSHR, and capturing their characteristics is key to achieve accurate predictions. Three-dimensional visualizations (Figure 1, right) indicated that PSHR takes place in the fuel-lean region at first due to relatively higher gas temperatures, and its effect becomes more significant in the more reactive fuel-rich region as time advances. The team also investigated effects of fuel properties such as laminar flame speed and heat of vaporization. The learnings from the fuel property study were used to explain some of the differences in PSHR behavior between Co-Optima alkylate and E30, based upon their chemical and physical characteristics.

By developing a modified set of best practices on how to capture the kinetic phenomena leading to knock under boosted operating conditions, this investigation provides a tangible step forward towards predictive simulations of knock in ICEs.

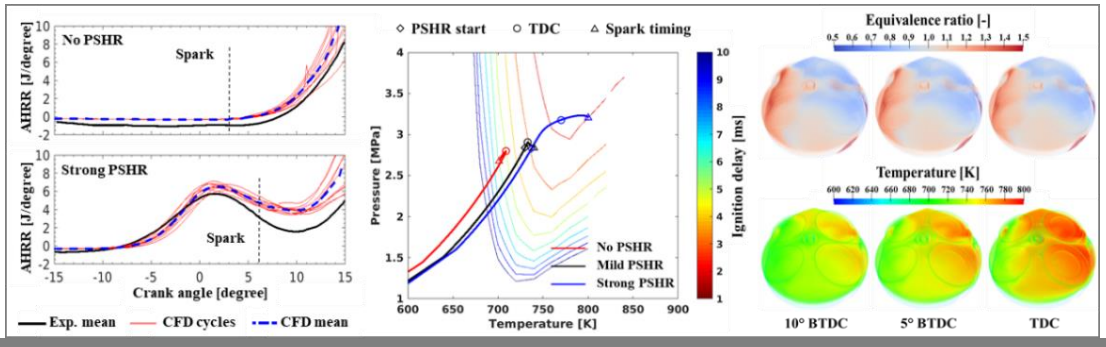

Figure 1. Left: Experimental and predicted apparent heat release rates under two conditions. Middle: In-cylinder P-T trajectories overlaid on the first-stage ignition delay contour. Right: 3D visualization of in-cylinder characteristics reveals the dynamics of PSHR..

2020 U.S. DRIVE Highlight

Gasoline Surrogate Formulation Developed for PACE Experiments and Engine Simulations

A concerted effort to match both the physical and chemical properties of a target E-10 market gasoline, validated by actual engine performance.

Argonne, Lawrence Livermore, Oak Ridge, and Sandia National Laboratories

A shared gasoline surrogate (Figure 1), which is a simplified mixture of representative fuel components, is needed to simulate a regular grade E-10 research gasoline for a diverse set of engine experiments within the Partnership to Advance Combustion Engines (PACE). Consortium tasks were crafted to meet U.S. DRIVE and Advanced Combustion and Emission Control Technical Team engine design and calibration goals. DOE laboratory expertise and capabilities were mustered to rapidly design a surrogate to match the target E-10 gasoline properties.

The surrogate optimization framework implemented at Lawrence Livermore (LLNL) and Sandia National Laboratories (SNL), reflecting additional input from PACE members, was used to target over 30 fuel properties and metrics for an initial surrogate designated PACE-1. In the Oak Ridge National Laboratory (ORNL) single-cylinder engine, PACE-1 matched the knock-limited phasing of the E-10 gasoline. PACE-1 also reasonably captured combustion phasing (Fig. 2) and emissions in the ORNL single cylinder engine under cold start conditions. These measurements, and others, of PACE-1 from consortium members and collaborators, were used to inform refinements leading to the final fiscal year 2020 surrogate recommendation, PACE-20. The optimization process matched research octane number and motor octane number within 0.3 octane units without significantly compromising other target properties. The distillation properties of the E-10 gasoline were reasonably captured. Spray penetration, collapse, morphology, and the onset of flash boiling as measured at SNL were captured well using the PACE-20 surrogate. Simulated laminar flame speeds of the PACE-20 surrogate using the LLNL kinetic model matched well with measurements of the E-10 gasoline from University of Central Florida. In SNL's homogeneous charge compression ignition engine and Argonne National Laboratory's rapid compression machine tests, the PACE-20 surrogate captured combustion trends well. The PACE-20 surrogate was found to perform well over the diverse set of experimental and computational research addressing PACE major research outcomes.

Figure 1. A shared gasoline surrogate to inform PACE major outcomes by cross-cutting analysis of experiments and simulations.

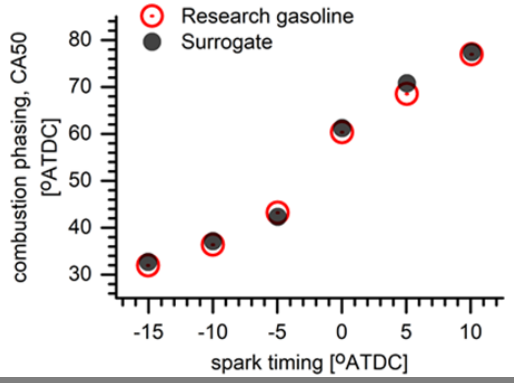

Figure 2. Initial PACE-1 surrogate (PACE-20 should be as close) reasonably captures combustion phasing in ORNL single cylinder engine under cold-start conditions (coolant, oil and air intake temperature, 20 °C).

2020 U.S. DRIVE Highlight

Co-Optima Develops Methodology to Quantitatively Value Fuel Properties for Efficiency Potential

A methodology to provide a guide for the development of emerging fuels from biomass or other feedstocks and serves as a capstone publication for the Co-Optima boosted spark ignition engine focus.

Co-Optima Initiative

The initial thrust of the Co-Optimization of Fuels & Engines (Co-Optima) initiative was focused on boosted spark-ignition (SI) engines. A newly released journal article in *Progress in Energy and Combustion Science* provides the scientific basis and a quantitative methodology to value fuel properties on the basis of the potential to increase engine efficiency. This capstone Co-Optima publication represents a joint effort across the Co-Optima initiative and includes 14 contributing authors from 4 national laboratories (Oak Ridge, Argonne, and Sandia National Laboratories; and the National Renewable Energy Laboratory).

This methodology considers six distinct fuel properties. The first four properties affect in-cylinder performance: research octane number (RON), octane sensitivity (S_{octane}), heat of vaporization (HoV), and flame speed (S_L). The last two properties, particulate matter index (PMI), and catalyst light-off temperature (Tc,90), affect engine efficiency through aftertreatment requirements. The unique impact that these properties have on efficiency is quantified for knock mitigation, dilution tolerance, low speed preignition, and aftertreatment. The result of this research is a unified merit function that normalizes the potential contribution of each fuel property in an optimized engine. Figure 1 shows a sensitivity analysis illustrating the potential contribution of the four fuel properties effecting in-cylinder performance. The fuel property with the largest potential impact on efficiency is RON, with S_{octane} being of a similar magnitude for boosted engines, but not for naturally aspirated engines. The sensitivity analysis also illustrates that the efficiency potential of HoV and S_L are small compared to RON and S_{octane} for stoichiometric SI engines.

This methodology allows new fuels being developed from biomass or other feedstock to be evaluated for efficiency potential on the basis of critical fuel properties, and can accelerate the development of emerging biofuels. Within the Co-Optima initiative, this approach has dramatically changed how biofuel researchers think and talk about fuels.

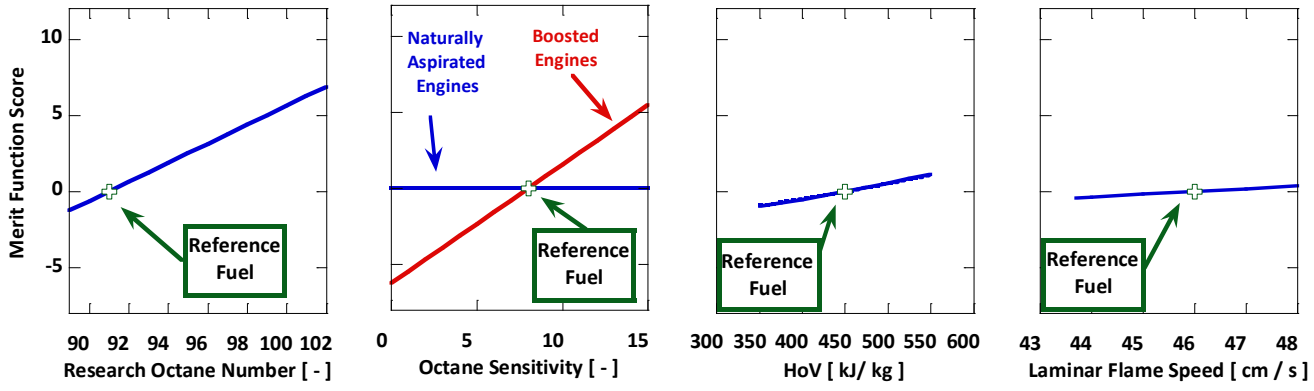

Figure 1. Sensitivity analysis of the merit function to four of the individual fuel properties considered, where higher values indicate a higher efficiency potential. Complete text of this capstone Co-Optima publication can be found at https://doi.org/10.1016/j.pecs.2020.100876.

2020 U.S. DRIVE Highlight

A Power Density High Efficiency Gasoline Lean Combustion Engine

Develop a gasoline low temperature combustion system which shows low fuel consumption and low emissions without deteriorating vehicle performance.

General Motors LLC

The primary objective of this program is the development and demonstration of a downsized boosted, lean, low temperature gasoline combustion (LTC) engine system capable of demonstrating a 15%-17% fuel economy improvement relative to a contemporary naturally aspirated stoichiometric combustion engine consistent with relevant emissions constraints and the use of marketplace gasolines. The program focused on maximizing internal combustion engine fuel economy potential by combining the benefits of downsized boosted engine technology with next-generation gasoline lean-burn, low temperature combustion.

General Motors successfully completed all technical deliverables through the end of the project. A summary of accomplishments during the project is stated below.

1. Developed homogeneous stoichiometric spark-ignition combustion and control for baseline reference.
2. Developed low temperature combustion and control including lean limit extension strategy during negative valve overlap (NVO) operation, stability improvement strategy during positive valve overlap (PVO) operation, LTC operating range extension strategy.
3. Developed combustion mode switching (transition) strategy including two-step cam lobe design, variable injection strategy to reduce combustion noise, and re-firing strategy after decel fuel cut-off (DFCO).
4. Develop emissions control strategy using low-cost passive selective catalytic reduction system.
5. The main enablers of this project are successful development of combustion phasing control strategy, noise reduction strategy during transient, mode switching strategy using physics-based control, and aftertreatment control strategy. In addition, the maximum extension of lean operation contributes to maximize fuel economy benefit (see Figure 1. 86% of Federal Test Procedure [FTP] cycle was operated in lean condition).

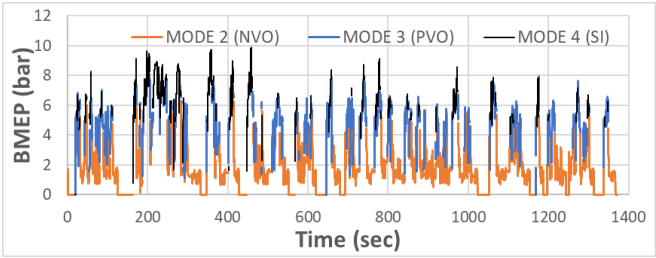

Figure 1. Variation of combustion mode during FTP cycle.

Summary of tail-pipe emissions of LTC engine obtained from hot FTP and cold FTP are shown in Figure 2. The project team met the SULEV 30 target for both hot FTP and cold FTP cycle test while achieving fuel economy gain of 20.5% and 18.9% respectively using degreened catalysts.

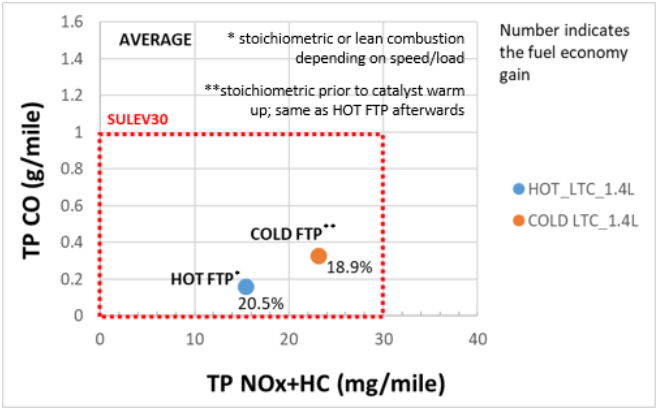

Figure 2. Summary of tail-pipe emissions results obtained from hot FTP cycle and cold FTP cycle test including fuel economy gain (averaged results of 3 measurements).

These technologies are part of a solution that is technically capable of introduction in the U.S. in the near- to medium-term and is consistent with current and anticipated future emission standards.

2020 U.S. DRIVE Highlight

Study Affirms Fuels with High Octane Sensitivity Outperform those with Low Sensitivity at High Loads and Speeds

Increasing octane sensitivity for fuels with RON ≥ 97 does not cause MON to become limiting in boosted engines.

Oak Ridge National Laboratory

Fuel anti-knock properties including research octane number (RON), motor octane number (MON), and the difference between RON and MON, known as octane sensitivity (OS), are key fuel characteristics that strongly influence spark ignition engine efficiency. Increasing RON and OS can improve engine efficiency by allowing the use of increased compression ratio. Increasing OS comes at the expense of lower MON, and there is not a full understanding of required MON levels at higher compression ratios. This study aimed to provide information about high load and high speed performance when MON is decreased relative to RON to provide greater OS for fuels with RON ≥ 97.

Fuels with RON ≥ 97 and OS ≥ 10 and isooctane, a fuel with OS = 0, were used in a turbocharged engine with a compression ratio of 12.4. The team compared maximum brake mean effective pressure (BMEP) and combustion phasing (CA50) when these fuels were used (Figure 1). At speeds up to 4,000 RPM, the 97 RON fuels with OS greater than 10 provided more advanced CA50, by up to 8 crank angle degrees (CAD). The more advanced CA50 provides greater engine efficiency and can enable greater BMEP. The experimental data were augmented by results using kinetic modeling to show that the high OS fuels continue to provide improved performance at up to 6,000 revolutions per minute (RPM) and when intake air temperatures rise to as high as 100°C, as might be experienced during high-power events in high-temperature ambient conditions. Thus, even at the high speed engine operating conditions with elevated operating temperatures, fuels with high OS continued to be beneficial for engine efficiency and a MON limitation was not encountered for fuels with RON and MON consistent with a premium or higher fuel grade.

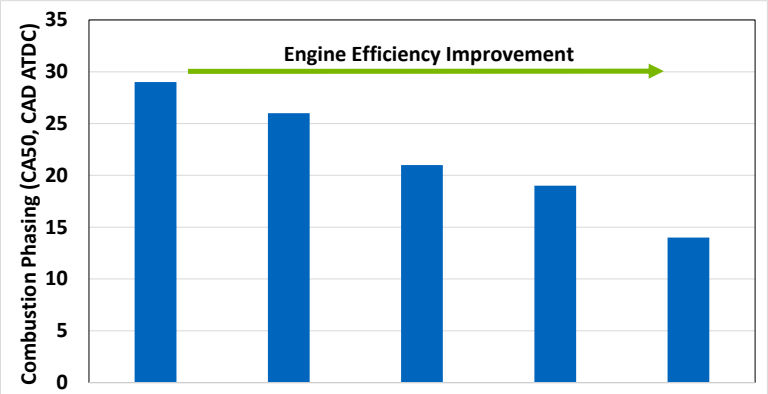

	Isooctane	Co-Optima Aromatic	Diisobutylene Blend	Co-Optima E30	E20 Blend
RON	100	98.0	98.2	98.3	101.3
MON	100	87.3	88.0	87.6	88.8
OS	0	10.7	10.2	10.7	12.5

Figure 1. Fuels with high OS enabled more advanced combustion phasing and thus higher efficiency at 4,000 RPM and 16 bar BMEP conditions compared to isooctane, which has OS = 0. Differing fuel chemistry produces different CA50 phasing at the same OS, pointing to the importance of chemical kinetics during the combustion process.

2020 U.S. DRIVE Highlight

Highly Efficient Palladium PNA for NO_X Control Enabling SULEV 30 Emission Compliance

Adsorbate-controlled location of atomically dispersed Pd(II) in Pd/FER passive NO_x adsorbers determines high activity and stability.

Pacific Northwest National Laboratory, BASF

Eliminating toxic nitrogen oxides (NO_x) emissions from internal combustion engines is necessary for societal and legislative purposes. Ammonia selective catalytic reduction (NH_3-SCR) technology successfully removes NO_x at greater than 200°C using sacrificial ammonia to drive the reaction and was implemented by BASF at large scale via Cu/SSZ-13. However, at low temperatures, less than 180°C, e.g., during vehicle cold start, current catalysts are incapable of performing this reaction effectively. Furthermore, ammonia cannot be delivered successfully to the catalyst at temperatures less than 180°C with urea as the source. To address the low-temperature cold start problem, palladium (Pd)/zeolite materials were introduced as passive NO_x adsorbers (PNA).

PNAs exhibit complex chemistry on single-atom Pd sites that must be further understood under practically relevant exhaust gas feeds if PNAs are to be a viable option for NO_x control. Despite their promise, there remains a formidable challenge for these materials to (1) be hydrothermally stable to 800°C, (2) perform well with elevated levels of carbon monoxide (CO) during cold start, and (3) exhibit excellent performance during consecutive PNA cycles and be regenerable.

Pacific Northwest National Laboratory (PNNL) and BASF researchers have discovered that treatment with high CO concentration results in a superior Pd/ferrierite (FER) zeolite PNA that yields greater NO_x storage and is more durable (Figure 1). Both Pd/FER and Pd/SSZ-13 benefit from the exotherm resulting from the oxidation of large amounts of CO. However, with Pd/FER researchers discovered that exposure to high CO concentrations induces Pd relocation resulting in a highly active PNA with high hydrothermal stability through 800°C. Then remarkably, under cold-start conditions, high levels of CO help move Pd into an active position for PNA. We observed the most hydrothermally stable and active ~2 wt% Pd/FER material in which the majority of Pd is atomically dispersed and available to NO_x storage. It shows good performance with repeated cycling, improving upon limitations associated with prior technology. Thus, by positioning Pd into specific locations in the FER, we have produced very hydrothermally stable and active PNA materials with practical applications.

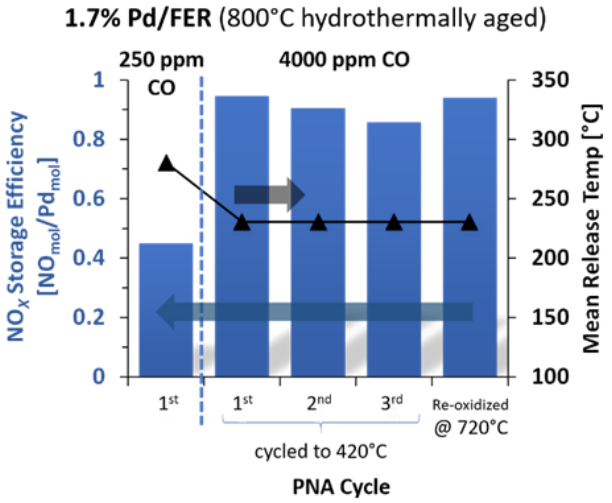

Figure 1. PNA performance of Pd/FER (Si/Al ~10) including NO_x storage efficiency & NO_x release temperature, with 220ppm NO_x, 14% O_2, 3 % H_2O and varying CO. The data includes comparison with 250ppm CO versus 4000ppm CO, and the results of 3 cycles with 4000ppm CO through 420°C compared to re-oxidation at 720°C in air.

Electrical and Electronics

2020 U.S. DRIVE Highlight

High-Speed Hybrid Reluctance Motor Utilizing Anisotropic Materials

Three motor variants demonstrate potential for heavy rare-earth-free traction motors.

General Motors

High cost and volatility are driving efforts to decrease reliance on the critical heavy rare-earth (HRE) materials used in traction drive applications. To that end, General Motors (GM) developed three variants of HRE-free electric motors: an HRE-free permanent magnet reluctance motor, a synchronous reluctance motor utilizing small HRE-free permanent magnets, and an induction motor with inserted copper bars and cast aluminum end rings. The designs take advantage of advanced magnet technologies and new topologies to improve mechanical strength and achieve power targets. The motors were designed for primary or secondary traction applications, depending on the topology.

Variant 1 achieved performance comparable to HRE-containing permanent magnet motors through optimized topology, as well as validated HRE-free magnets, focusing on achieving energy products and demagnetization resistance comparable to those of HRE-containing magnets. Demagnetization testing demonstrated the motor's robustness to currents and temperatures exceeding expected vehicle conditions, a key challenge to the use of HRE-free magnets. The Variant 1 motor also showed the best capability of meeting the U.S. DRIVE technology targets, owing to the high power density of the permanent magnet motor and the potential cost reductions enabled by the removal of HREs. Performance of the Variant 1 motor at the nominal 350 volt (V) is shown in Figure 1.

Variant 2 exhibited high efficiency in high-speed regions because of the low high-speed losses, an important consideration for secondary traction applications, and significantly thrifted on magnet mass to reduce cost.

Variant 3 contained copper bars within the induction rotor to reduce losses compared to cast aluminum, while using cast aluminum end rings to reduce the cost and mass of the rotor. Researchers focused on optimizing the copper–aluminum interface, which is prone to forming brittle intermetallic compounds.

Prototypes of each motor variant were built and tested for performance, mechanical strength, and demagnetization resistance (Variants 1 and 2 only), with torque and power close to predicted values. Table 1 provides the testing results.

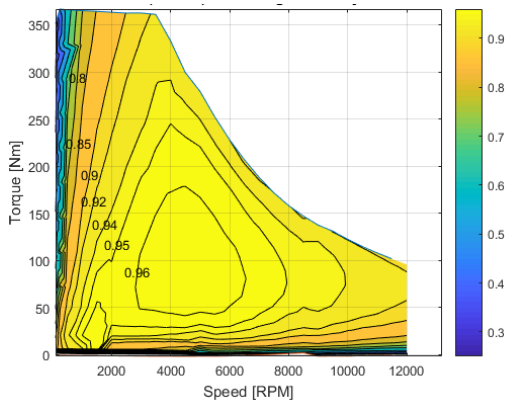

Figure 1. Performance results of the Variant 1 motor, tested at 350V.

	Variant 1	Variant 2	Variant 3
Stator Outer Diameter	208 mm	190 mm	190 mm
Rotor Outer Diameter	139.5 mm	139.1 mm	139.1 mm
Stator Core Length	200 mm	100 mm	100 mm
Power	148 kW	86k W	84 kW
Torque	372 N-m	249 N-m	310 N-m
Max RPM	12,000	16,500	14,000

Table 1. Comparison of each motor variant. Packaging size was selected based on the intended application of each motor variant.

2020 U.S. DRIVE Highlight

Experimentally Confirmed High Thermal Performance of the Novel Dielectric Liquid Cooling Concept

Concept predicted to enable achieving power density of 100 kW/L, a U.S. Department of Energy 2025 target.

National Renewable Energy Laboratory

The National Renewable Energy Laboratory (NREL) has developed a novel cooling concept that is predicted to provide better thermal performance than current automotive technology, thereby increasing the power density of electronics to as much as 100 kW/L. Higher power density translates into better performance but is limited by heat generated during operation. NREL's cooling concept uses single-phase dielectric liquid jets impinging on a densely finned heat spreader surface to cool the devices indirectly. Although dielectric fluids have poor properties (e.g., high viscosity at low temperatures) compared to the coolant commonly used in automotive applications, these liquid materials allow for a redesign of the power module to eliminate the ceramic dielectric layer, which can lower overall thermal resistance, improve reliability, and reduce cost. Dielectric fluids also offer the ability to cool the electrical interconnections directly, which can decrease capacitor and gate driver temperatures and enable more compact packaging (i.e., high power density).

NREL used computational fluid dynamics (CFD) modeling to design a jet impingement-based dielectric fluid cooling system. Modeling predicts a low junction-to-fluid thermal resistance (21 mm²·K/W) and low pumping power (0.15 W), which are 50% and 80% lower, respectively, than the 2015 BMW i3. A prototype of the cooling concept was fabricated out of lightweight and low-cost plastics using additive manufacturing methods (Figure 1). Researchers conducted experiments to measure the heat exchanger thermal resistance and pressure drop at various fluid flow rates and temperatures using Alpha 6 fluid, a dielectric and heat transfer oil for applications with very high operating temperatures. The experiments confirmed the low thermal resistance and low pumping power requirements predicted by the CFD model (Figure 1).

The good match between the modeling and experimental results confirmed the model's predictive abilities. NREL then used the model to evaluate several dielectric fluids (AC-100 and automatic transmission fluid) at various fluid flow rates and temperatures (-40°C to 70°C). The model results predict that using AC-100 at -40°C can provide both a lower junction-to-fluid thermal resistance and lower pumping power requirements compared with the 2015 BWM i3 at 65°C. These results suggest that dielectric fluid viscosity concerns may not be an issue if the correct low-viscosity fluid is selected and combined with a low-pressure-drop heat exchanger. Next steps include modeling a double-sided concept and experimental implementation within a package/module.

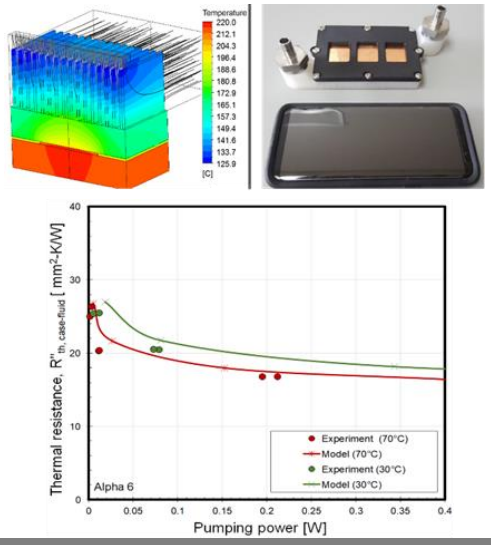

Figure 1. Model results showing temperature contours and fluid streamlines (top left); image comparing the cooling system's size to that of a cell phone (top right); graph showing a good match between model and experimental results at various fluid flow rates and temperatures (bottom).

2020 U.S. DRIVE Highlight

Graphite Embedded High-Performance Insulated Metal Substrate for Wide Bandgap-Based Power Modules

Developed and experimentally validated steady-state and transient thermal performance of graphite embedded insulated metal substrates to replace conventional direct bonded copper solutions.

Oak Ridge National Laboratory

A high-performance substrate was developed in collaboration with Henkel and Momentive to provide high-performance thermal management for wide bandgap (WBG) power modules. With increased power loss density in a WBG-based converter and reduced die size in power modules, thermal management of power devices must be optimized for high performance. The proposed graphite-embedded substrate's electrical performance is validated with static and dynamic thermal characterization. Using graphite-embedded substrates instead of direct bonded copper (DBC) substratse, the junction-to-case thermal resistance of silicon carbide (SiC) MOSFETs can be reduced up to 17%, and device current density can be increased by 10%, regardless of the thermal management strategy used to cool the substrate. Reduced transient thermal impedance of up to 40% due to the increased heat capacity is validated in transient thermal simulations and experiments. The half-bridge power module's electrical performance is evaluated for on-state resistance, switching performance, and switching loss at three different junction temperature conditions. The proposed substrate has minimal impact on conduction and switching performance of SiC MOSFETs.

The insulated metal substrate with thermal pyrolythic graphite (IMSwTPG) is formed by an insulated metal substrate (IMS) with multiple conductive and dielectric layers to accommodate the half-bridge configuration for a typical power module. The structure of the substrate is presented in Figure 1. The top layer provides the connection for gate terminals and DC connection. The SiC MOSFET dies are attached to the copper cores with embedded TPG tiles and separated from each other with a dielectric separator, and from the top and bottom layer with thin polymer dielectric layers with relatively high thermal conductivity. The bottom layer is attached to the cold plate for extraction of the heat generated in SiC MOSFETs during operation of the power converter. Furthermore, due to construction flexibility of IMSwTPG structure, the bottom layer can be designed as an integrated high-performance heat sink to eliminate the interface between the substrate and the cooling structure for enhanced thermal management.

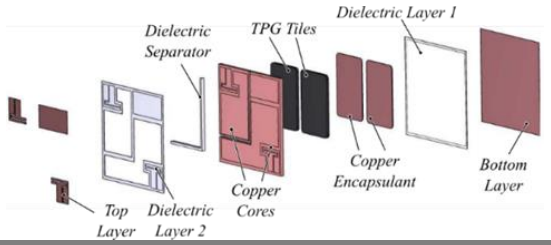

Figure 1. Structure of the graphite embedded insulated metal substrate.

The fundamental objective of the graphite is to spread the heat generated in the SiC MOSFET dies across the core to utilize the surface area of the core before reaching the dielectric layer in the thermal management network. This will enhance the heat transfer area for the substrate and hence reduce the junction-to-case thermal resistance of SiC MOSFETs. For this purpose, the anisotropic properties of the TPG are utilized to spread the heat by aligning high thermal conductivity planes of the TPG tiles. The in-plane alignment provides spreading of the heat generated in SiC MOSFET dies to the power and gate terminal areas on the substrate where the heat flux is relatively low. From the design perspective, this is achieved by expanding the TPG tile underneath the terminal regions using the three-layer structure in the IMSwTPG (see Figure 1). Furthermore, the proposed alignment of the TPG tile will limit the heating interaction between paralleled dies due to low thermal conductivity in that axis.

2020 U.S. DRIVE Highlight

Co-Optimization of Boost Converter Reliability and Volumetric Power Density

Research team uses a genetic algorithm to evaluate multi-objective trade space and optimize designs.

Sandia National Laboratories

Electric drive system performance is improved through innovation in semiconductor devices, passive component materials, and thermal management technologies between power electronics and electric motors. However, such tightly integrated systems require comprehensive analysis to identify the factors driving reductions in cost, volume, and weight while simultaneously increasing efficiency and reliability.

Sandia National Laboratories has utilized multi-objective optimization to analyze the reliability and power density of a boost converter, a device that increases voltage in an electric drive system. The simplicity and ubiquity of the circuit make it a useful test case for evaluating the optimization approach's accuracy. Sandia employed a genetic algorithm—a population-based evolutionary search technique—to investigate design trade-offs between various component materials and cooling techniques.

Figure 1 depicts pareto-optimal solution sets that evaluate power density and mean time between failure (MTBF) (the predicted time between inherent system failures) for a 5 kW boost converter using different magnetic component types. The figure illustrates the trade-offs due to the varying magnetic properties and loss characteristics in different inductor core materials. Moreover, similar approaches have been taken for cooling mechanisms, semiconductor devices, and capacitor materials.

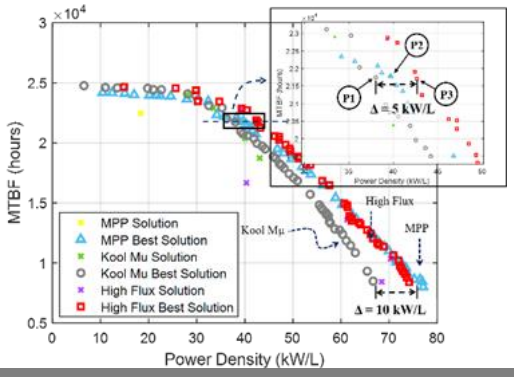

Figure 1. Pareto solution evaluating Kool Mμ, High Flux, and Molypermalloy Powder (MPP) and the prototypes with different inductors denoted as P1, P2, and P3.

Figure 2. Picture of the hardware prototype with the High Flux core design, P3.

Figure 2 shows a hardware prototype that was constructed to demonstrate and verify the design operating points. Figure 3 illustrates good agreement between the experimental results and the simulated behavior of the converter.

This work provides a foundational platform that can be used to optimize additional power converters, as well as trade-offs in thermal management due to the use of different device substrate materials.

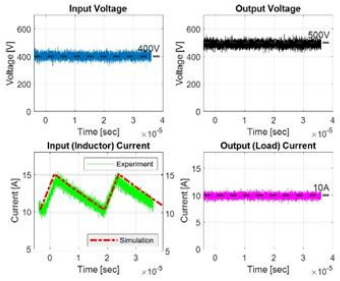

Figure 3. Measured waveforms of the 5 kW boost converter operation with input of 400 volt (V)and output of 500V for the High Flux design, P3

Electrochemical Energy Storage

2020 U.S. DRIVE Highlight

A Lithium-ion Battery Electrolyte Recycling Process

Recovering electrolytes during Li-ion battery recycling could have a positive impact on revenue and therefore make recycling more viable and profitable. ReCell has developed a recycling process that can recover the $LiPF_6$ salt and some other electrolyte components for re-use, with resulting performance similar to that of a baseline electrolyte.

Argonne National Laboratory

Creating a profitable lithium (Li)-ion battery recycling process will enable a comprehensive recycling program and reduce the cost of batteries using these recycled materials. Maximizing revenue requires that as many components as possible be recovered. One such opportunity is to recover the electrolyte and its relatively expensive Li salt, $LiPF_6$.

A recycling process for end-of-life Li-ion batteries typically starts with shredding (Figure 1a). At this point the recovered shredded material is coated with the liquid electrolyte. This electrolyte must be removed before further processing because it contains $LiPF_6$ that can react with other materials. Utilizing a low boiling point carbonate solvent such as dimethyl carbonate or diethyl carbonate, the electrolyte is removed from the solid shreds. The recovered materials contain a complex mixture of carbonates and decomposition products as can be seen in Figure 1b.

The recovered electrolyte is too dilute for use, so that material was concentrated via evaporation. Evaporation removed many of the contaminants from the electrolyte. After the evaporation process a new electrolyte was formulated using the remaining ethylene carbonate and $LiPF_6$. After performing this process on an end-of-life commercial battery, the recycled electrolyte was tested in a full cell to see if it performed as well as a pristine electrolyte. The resulting cycling data are shown in Figure 1c. The recycled electrolyte shows more rapid initial capacity fade, but in longer term cycling it has a lower fade rate than the pristine electrolyte. The improvements are likely due to trace levels of additives, such as $LiPO_2F_2$, that remain after recovery. These data indicate that electrolyte can be recovered from spent Li-ion batteries with performance comparable to the virgin electrolyte.

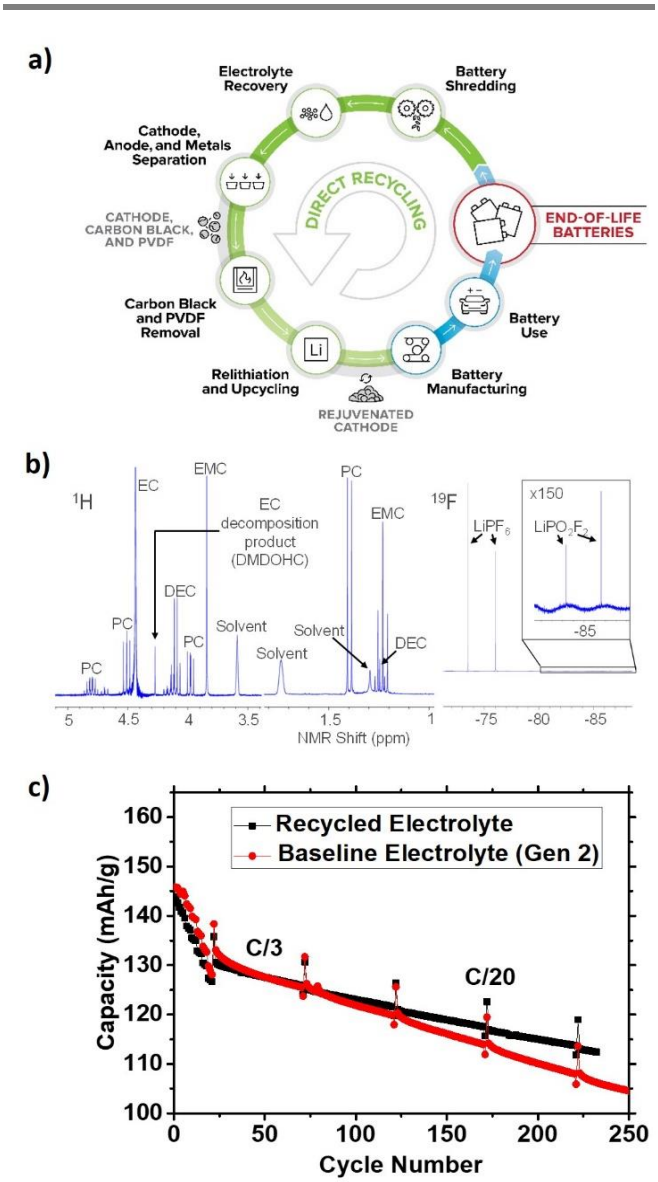

Figure 1. (a) Schematic diagram of a direct recycling process. (b) ^{1}H and ^{19}F NMR spectra of recovered electrolyte from a commercial cell. (c) Cycling of $LiNi_{0.33}Mn_{0.33}Co_{0.33}O_2$ versus graphite using a recycled electrolyte and a baseline electrolyte.

2020 U.S. DRIVE Highlight

Highly Uniform Dopant Distributions Improve Life in High-Energy Nickel-Rich Cathodes

Novel processing utilizing atomic layer deposition provides a higher degree of control over dopant distribution compared to typical routes—resulting in enhanced electrochemical performance.

Argonne National Laboratory

Layered $LiNiO_2$ and its substituted derivatives (>~90% nickel [Ni]) have been studied for many years as lithium-ion cathodes due to their high energy densities and low cobalt contents. However, thermal and structural instabilities make it clear that modifications (i.e., dopants) are critical to using these oxides in commercial cells. Though compositions such as aluminum (Al)-containing NCAs have found success, recent work from Argonne National Laboratory (ANL) has shown that even NCA-type commercial oxides can have inhomogeneous distributions of Al.[1] Therefore, improvements in Ni-rich oxide performance might be expected through more advanced processing.

Figure 1(a) shows ^{27}Al nuclear magnetic resonance (NMR) spectroscopy results of two cathodes of the same composition, $LiNi_{0.92}Co_{0.06}Al_{0.02}O_2$. However, one oxide was doped with Al using typical wet-chemical processing and one was doped by deposition of Al on NiCo-hydroxide precursors through careful control of atomic layer disposition (ALD) parameters. The major findings revealed that wet processing resulted in ~20% of the Al incorporated in surface phases (Al_2O_3 and $LiAlO_2$); however, the ALD processing resulted in all Al incorporated into bulk-like lattice sites. High-resolution microscopy (Pacific Northwest National Laboratory) verified a uniform distribution of Al within the particles. Figure 1(b) shows that the wet-chemical processing did improve the cycling stability of the undoped baseline, however, the uniform Al distribution of the ALD sample resulted in a 5%–6% improvement in capacity retention. Recent related studies also show that other ALD-doped oxide compositions show higher onset temperatures for phase transitions in charged electrodes. Furthermore, ALD-doped oxides have shown enhanced resiliency to surface impurities towards potential improvements in storage stability of Ni-rich NMCs.

The results herein indicate that Al^{3+} cations incorporated into fully coordinated lattice sites have a larger impact on cathode stability than surface Al phases. It is also clear from this work that achieving the greatest benefit from substitutions requires a high degree of control over distribution and site occupancies. The novel, ALD processing developed at ANL could be a viable option. This method is expandable over the vast library of ALD precursors including the possibility of multiple-dopant compositions for bulk/surface stabilization.

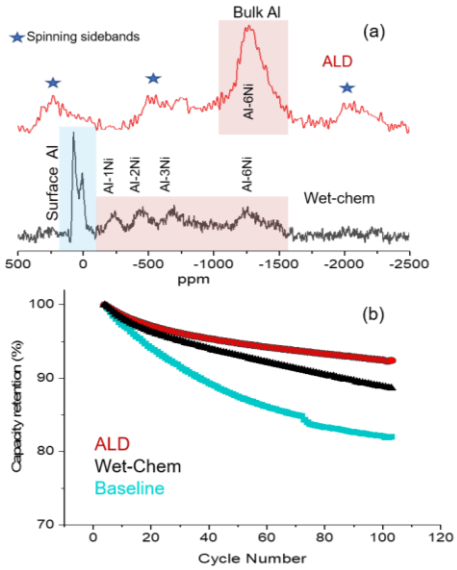

Figure 1. (a) NMR spectroscopy of Al environments from ALD and wet processing. (b) Capacity retention of Al-doped samples compared to the undoped baseline in half cells. All samples had similar initial capacities of ~230 mAh/g, 4.4 volt (Li/Li^+), 30°C.

[1] Dogan, F. et al, ACS Appl. Mater. Interfaces 2016, 8, 16708–16717.

2020 U.S. DRIVE Highlight

Pushing the Limits of Rechargeable Lithium Metal Battery Cycle Life and Energy Density

Battery500 Consortium researchers integrated materials science, electrochemistry, and engineering to extend the cycle life of high-energy lithium metal batteries.

Battery500 Consortium

The Battery500 Consortium pushes the frontier of advanced electrode and electrolyte materials and develops strategies to integrate materials science, electrochemistry, and cell engineering in high-energy rechargeable lithium (Li) metal batteries to achieve more than 400 cycles in prototype 350 Wh/kg pouch cells (2 Ah) (Figure 1a–b).

To decelerate the continuous side reactions in Li metal batteries and the consumption rate of both lean electrolytes and thin Li in realistic pouch cells, a localized concentrated electrolyte consisting of 1.54M lithium bis(fluorosulfonyl)imide (LiFSI) in 1,2-dimethoxyethane (DME) and 1,1,2,2-tetrafluoroethyl-2,2,3,3-tetrafluoropropyl ether (TTE) has been developed to minimize the formation of "dead" Li formed during cycling and improve the efficiency of Li deposition/stripping. The properties of solid electrolyte interphase layers formed between the newly developed electrolyte and Li metal are also improved, minimizing the amount of electrolyte irreversibly consumed during cycling.

To accelerate mass transport, high mass-loading cathode architectures with controlled porosities are coupled with a Li anode (Figure 1c-d) to increase Li^+ diffusion and reduce opportunities for spiky microstructures of Li to form during cycling. The synthesis conditions and electrochemical properties of high nickel manganese cobalt oxide cathodes are investigated to balance capacity and cycling stability.

A new, user-friendly software for designing Li metal batteries has been developed, see https://www.pnnl.gov/technology/li-batt-design.app, to derive the key cell parameters needed to achieve the desired cell-level gravimetric and volumetric energy densities. Standard Battery500 coin cell testing protocols have been developed and implemented to compare and select the materials or approaches developed within the Consortium and from collaborators. The Consortium has used advanced in situ and ex situ characterization techniques—such as cryogenic electron microscopy and in situ X-ray diffraction—to monitor and quantify the chemical and structural changes of electrodes, providing feedback on pouch-cell-level design.

New knowledge gathered from cell degradation mechanisms, as well as the combination of cell design, compatible interfaces, and uniform initial pressure applied on the cell, 26.7 psi, synergistically extends the stable cycling of 350 Wh/kg pouch cells with 80% capacity retention after 430 cycles, Fig 1.

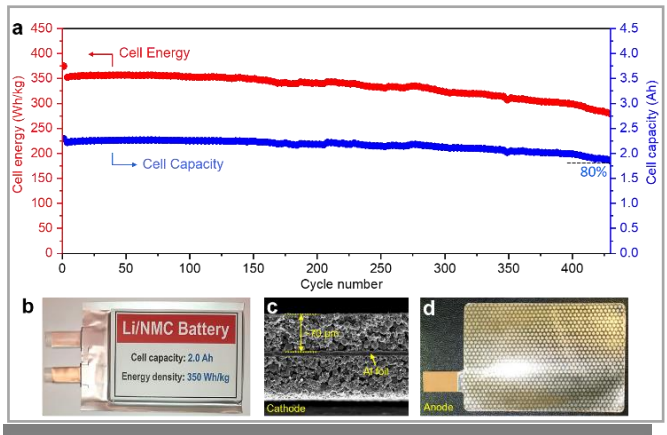

Figure 1. 350 Wh/kg pouch cells achieve more than 400 cycles. (a) Cell-level energy and capacity at different cycling. (b) Image of a 350 Wh/kg Li metal pouch cell developed at Pacific Northwest National Laboratory. (c) Structure of a $LiNi_{0.6}Mn_{0.2}Co_{0.2}O_2$ cathode coated on both sides of aluminum current collector. (d) One of the Li anodes incorporated in the pouch cell.

2020 U.S. DRIVE Highlight

Towards Higher-Energy Density via State-of-Charge Gradient Determination in Thick Electrodes

Researchers used synchrotron diffraction methods to quantify the vertical inhomogeneity in thick cathode films to understand the origin of the performance limitations in this energy-dense electrode.

Brookhaven National Laboratory

One generally applicable route for enhancing the energy density of lithium-ion batteries (thereby increasing the range of electric vehicles) is using thicker electrode (anode and cathode) films. However, the specific capacity and rate performance of thick electrodes is reduced due to limitations in the transport of ions and/or electrons perpendicular to the plane of the film. If the precise origin of these transport limitations can be understood, it might be possible to rationally design thicker electrodes that deliver higher energy densities than present batteries while still meeting the other performance demands of electric vehicles.

Researchers used high energy synchrotron X-ray diffraction methods to study the top-to-bottom inhomogeneity in the state of charge (SOC) of thick (170 micron) battery cathode films. The height of the X-ray beam was reduced to 20 microns, allowing thick cathode films to be virtually 'sliced' into about ten layers (much like a stack of postage stamps), enabling the performance of each layer within the whole cathode film to be independently followed during battery testing. The ability of the X-ray techniques to accurately measure the local SOC in a layer was confirmed by the agreement in the average response measured across all layers by X-rays (cyan line, Figure 1) to that measured conventionally using the potentiostat-controlled battery cycling (black line).

The next step was to compare the response from the back of the cathode layer (where the electrical contact with the current collector is made) to that of the front of the cathode (nearest to the anode). While layers in the front of the cathode behaved in the expected manner (Figure 2), it was observed that the back layers could store only about half of the capacity of the front of the cathode after a normal charging cycle at C/10, suggesting that the primary transport limitation is ionic and not electronic. Furthermore, researchers observed that when the discharge of the battery starts (time = 12 hrs, green arrow), the back cathode layers unexpectedly continue to charge for another hour, and in fact increase their SOC faster than at any point during the charging of the battery. The spatially resolved diagnostic methods demonstrated here are being used to parameterize models of cathodes that can better predict how battery design changes will affect performance. This novel technique provides a new look into potential pathways towards increasing battery energy density.

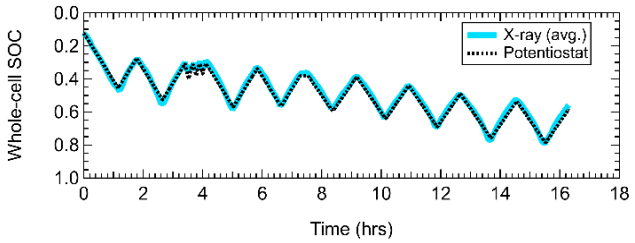

Figure 1. Comparison of the battery state of charge calculated from X-ray diffraction measurements (cyan) with that recorded using the potentiostat driving battery cycling (black).

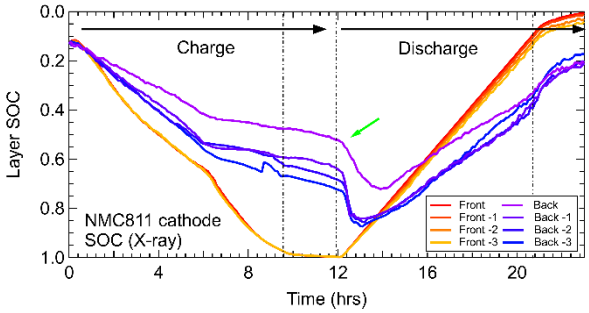

Figure 2. Comparison of the battery SOC for 4 layers at the top of the cathode (red-orange) and 4 layers at the back of the cathode (purple-blue).

2020 U.S. DRIVE Highlight

Lithium-Ion Cell Brings Extreme Fast Charging Closer to Reality for Electric Vehicles

A 35Ah lithium-ion pouch cell has been developed using advanced cell materials that can be charged in 10-minutes reproducibly more than 850 times.

Microvast, Inc.

The convenience of quickly refilling a car is one advantage of gasoline vehicles compared to fully electric alternatives (although home charging is arguably an advantage of electric vehicles [EV]). While fast charging EVs presents challenges to electricity grids and charging stations, perhaps the most difficult hurdles to overcome are from the lithium-ion (Li-ion) battery cell itself. During fast charge the high currents typically cause higher temperatures and uneven chemical reaction rates within the cells. These operating conditions in turn lead to faster cell degradation. Further, these degradations typically become more intense as the Li-ion cell energy density is increased.

One of the most straightforward ways to change a Li-ion cell's performance and energy density is by using different materials. Cell component material properties differ based on composition and physical attributes, which in turn influences the cell's performance. It is especially important to improve the cathode, the most expensive individual cell component. Higher capacity cathodes lead to more energy density, while improved properties slow cell degradation and resistance increases. Using the full concentration gradient (FCG) cathode technology that Microvast is developing for commercialization, cathodes with tailored surfaces that are more stable to fast charge effects were prepared. The FCG technology allows engineers to change the atomic composition of metals throughout the cathode particle, placing more desirable metal oxide combinations at locations most vulnerable to degradation. Also, as the nickel content of the FCG cathode is increased the prototype cell's C/3 energy density could be improved.

Initially, a 200 Wh/kg cell was the highest energy density cell made by Microvast that could achieve the 500 10-minute charging goals. Steadily that number has improved as the cathode was optimized, eventually reaching 240 Wh/kg as the base (0.33C) energy density, a 20% improvement. In Figure 1 the 10-minute charging (6C), 1-hour discharge (1C) cycle data for prototype 240 Wh/kg cell is shown compared to the project goals. Beyond 500 cycles the cell-to-cell variance does increase, but most cells achieve more than 1,100 cycles before reaching end of life. These results, collected from automotive relevant 35 Ah pouch cells, showcase that more than 1,000 10-minute fast charges is feasible for automotive relevant cells.

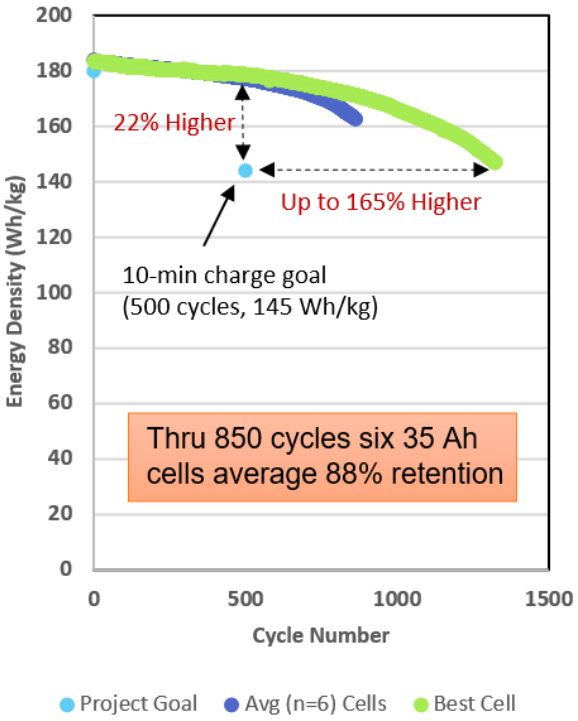

Figure 1. The energy density versus cycle number of tested 10-minute charge / 1-hour discharge Li-ion cells. The project energy density goals, average for 6-duplicate cells and the best cell tested is shown.

2020 U.S. DRIVE Highlight

Protocol for Early Assessment of Calendar Life and Faster Technology Development in Silicon-Based Anodes

Holding the voltage at top of charge for a silicon cell with excess lithium from the cathode can help predict calendar life with a dramatic reduction in required test time.

Silicon Consortium Project Team (Argonne National Laboratory, National Renewable Energy Laboratory, Oak Ridge National Laboratory, Sandia National Laboratories, Pacific Northwest National Laboratory, and Lawrence Berkeley National Laboratory).

Silicon (Si) anodes offer the prospect of lithium ion (Li-ion) cells with 30% improvement in energy compared to today's graphite anode cells. However, their short calendar life (2-3 years) is a major hurdle to commercialization. Calendar life testing of battery cells is traditionally carried out by aging cells for multi-month-long timeframes. Thus, development of a short-timeframe (days instead of months/years) calendar life test could enable faster feedback and development of new and improved materials.

The new electrochemical test provides a mechanism that researchers and developers can use to assess the progress in the development of Si-based negative electrodes within a short timeframe of two weeks. This test makes use of a constant voltage hold in a Li-excess full cell containing a Li iron phosphate counter electrode with a flat voltage output. The current passed during the voltage hold is a measure of the reaction rate of lithium consumption at the Si anode through parasitic and irreversible electrochemical reactions.

Figure 1 shows the current decays of three different Si test electrodes and a graphite baseline electrode. Tests were conducted in triplicate although just one data set is shown for clarity. The normalization of the current data to the reversible capacity of each electrode is important because the resulting units of Amps/Ah indicate the rate at which each electrode is losing reversible capacity due to Li^+ consumption at the solid electrolyte interphase (SEI). If the normalized current measured from a Si test electrode at the end of the 180 hour voltage hold is clearly higher than a baseline electrode, further analysis is not needed, as the electrode's SEI is not sufficiently stable. This is the case for each of the Si electrodes shown, thus showing the effectiveness of this comparison for the screening of Si electrodes.

Our methodology is based on using *voltage holds* to measure the rate of parasitic reactions that irreversibly trap Li^+ at the Si SEI. This approach has the advantage of recording real-time rates of side reactions, providing information about the time-dependence of such processes and potentially enabling extrapolation of behaviors observed in relatively short duration experiments. Indeed, a numerical model of the parabolic-like decay of the current is under validation using long-term voltage hold measurements. The long-term validation test will allow an accurate fit traced back to 180 h of Si calendar life testing.

Cathode/anode interactions may impact calendar life as well. Thus, in the future, this method may be expanded to incorporate additional cathodes.

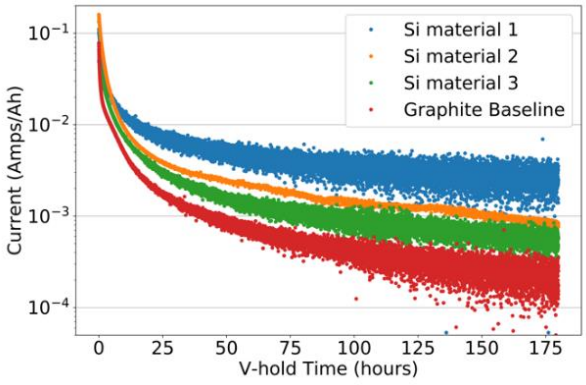

Figure 1. Current decay versus time during voltage holds of several different Si test electrodes and a graphite baseline electrode.

2020 U.S. DRIVE Highlight

Electrolyte Development for Extreme Fast Charging (XFC) of Lithium-ion Batteries

A high-performance electrolyte has been developed to increase lithium-ion mass transport during XFC, achieving 180 Wh/Kg energy density and maintaining > 80% energy density after 1000 XFC cycles.

Oak Ridge National Laboratory

Enabling fast charging of high energy density lithium-ion (Li-ion) cells could dramatically increase the widespread adoption of electric vehicles. However, fast charging is limited by Li ion depletion in the electrolyte and the accompanying Li plating over graphite anodes. One of the solutions for enabling extreme fast charging (XFC) while retaining high battery energy can be achieved through enhancing the Li ion mass-transport in electrolytes such that enough Li ions are available for intercalation in graphite.

Researchers at Oak Ridge National Laboratory (ORNL) have developed high performance electrolytes with optimized Li salt, solvents, and additives. The electrolytes have both higher Li ion conductivity and Li ion transference number, compared to state-of-the-art electrolyte. The electrolyte development is ideal for higher Li ion transport and has been identified as a significant step towards realizing cells with XFC capabilities.

The electrolytes were tested in 1.5Ah NMC622/ graphite pouch cells using the 6C (10 minute) charging protocol. The cell with ORNL V2 electrolyte retained 89% capacity after 500 XFC cycles (Figure 1), exceeding the targeted goal (80% after 500 cycles), and much better than the 64% retention for the Gen2 baseline electrolyte (1.2 M $LiPF_6$ in EC:EMC 30:70 wt%). Continued cycling of the cells show 80% capacity retention after 1000 cycles. The cell can have an energy density of ~180 Wh/Kg (when scaled up to 50 Ah), which meets the targeted goal for energy density. After 1000 XFC cycles, the cell still has 141 Wh/kg energy density. When the cell was charged/discharged at C/3 after 1000 XFC cycles, it can still deliver 193 Wh/kg.

Future work will include the understanding of high voltage holding during XFC and optimizing formation protocols for XFC of Li-ion cells.

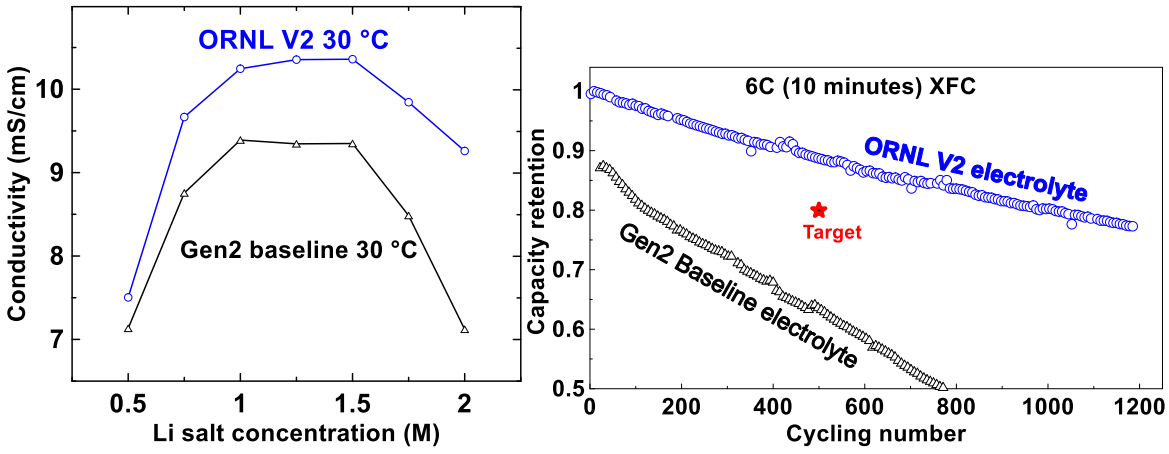

Figure 1. Left, conductivities of ORNL V2 and Gen2 baseline electrolyte. Right, capacity retention versus cycling number under 6C (10 minutes) XFC protocol with 2-Ah cells filled with ORNL V2 and Gen2 baseline electrolyte.

2020 U.S. DRIVE Highlight

Sustainable Direct Recovery of Battery Materials from Manufacturing Scraps

An environmentally friendly solvent-based separation process is developed to efficiently recover electrode materials and metal foils with no damage or corrosion.

Oak Ridge National Laboratory

Lithium-ion (Li-ion) batteries are valuable and recyclable, but recycling processes are costly. Profitable recycling of Li-ion batteries will thus depend on new process developments. Electrode materials are tightly bonded to their respective metal current collectors through polymeric binders. To recover electrode materials, especially cathode materials that represent the most recoverable value, an efficient and damage-free separation process needs to be developed to isolate electrode materials from metal foils like aluminum (the cathode current collector) and copper (the anode current collector).

Scientists at Oak Ridge National Laboratory (ORNL) have developed a solvent-based separation process to recover both electrode materials and metal foils without any damage and corrosion. Novel electrode recovery process based on a greener solvent, ethylene glycol, enables the delamination of electrode coatings from metal foils in few seconds (Figure 1a). The recovered battery materials tested to date, especially NMC cathodes, are damage-free in terms of crystal structure and microstructure and are equivalent to their pristine cathode counterparts in terms of electrochemical performance (Figure 1b). This separation process might be deployed in battery manufacturing plants ensuring that the electrode scraps (up to 10% of the total processed electrodes) can be treated onsite safely and reprocessed as new electrodes.

In addition to the reclamation of cathode materials, recovery of other materials such as graphite and metal foils provides an additional materials cost saving. Reclaiming copper and aluminum could greatly reduce emissions of sulfur oxides, nitrogen oxides, and energy consumption. As shown in Figure 1a, the recovered metal foils show no sign of corrosion or residues, providing a path for their reuse in battery manufacturing and for lessening the carbon footprint in mining and refining. Furthermore, the recovered graphite from anode scraps shows equivalent electrochemical performance as the baseline graphite (Figure 1c).

This robust separation process operates at a low temperature and is scalable. Ethylene glycol is a commodity with low toxicity and has an annual consumption of 20 million tons for use as antifreeze and polymer precursor. Moreover, ethylene glycol can be reused to close the recycling loop without generating secondary waste. Overall, the ethylene glycol-based separation is a sustainable electrode recovery process that greatly advances battery recycling.

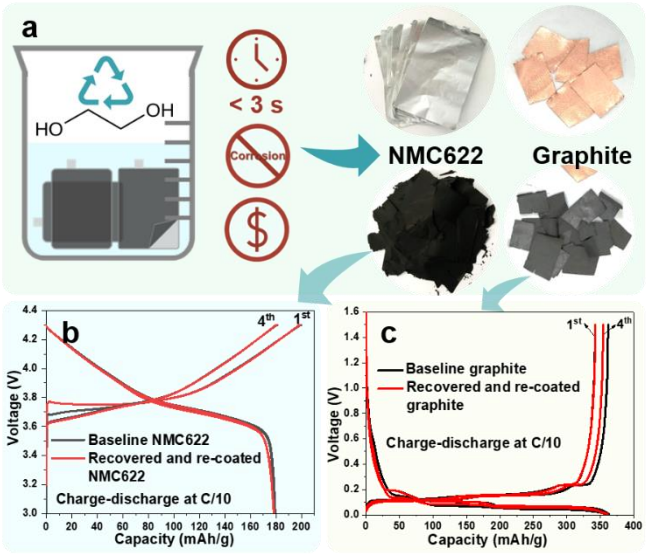

Figure 1. (a) Photos showing the recovered electrode materials and metal foils. 1st and 4th charge-discharge profiles for the recovered and re-coated electrodes of (b) NMC622 and (c) graphite at C/10 rates.

2020 U.S. DRIVE Highlight

Development of Silicon-Based High-Capacity Anodes for Next-Generation Lithium-Ion Batteries

Micron-sized porous silicon anode and localized high concentration electrolytes enabled long term cycling of high-capacity silicon-based lithium-ion batteries.

Pacific Northwest National Laboratory

Porous silicon (Si) has been widely used to mitigate pulverization of Si particles and accommodate swelling during battery cycling. However, the large surface area of these Si materials may lead to severe reactions between lithiated Si and electrolyte. These reactions lead to continuous growth of the solid electrolyte interphase layer and short cycle life and calendar life. Therefore, minimizing the surface area of Si and finding a stable electrolyte are critical for improved cycling and calendar life of Si-based lithium-ion batteries.

Researchers from the U.S. Department of Energy's Pacific Northwest National Laboratory (PNNL) have developed a stable Si anode based on micron sized porous Si with heterogeneous coating layers. Porous Si was first prepared by thermal decomposition of SiO and subsequent etching. It was then treated at low temperature to form an intermediate layer on porous Si. The treated porous Si was coated with carbon using petroleum pitch as carbon precursor. Si/NMC532 coin cells using the porous Si-C have demonstrated excellent performances using a baseline electrolyte (1.2M $LiPF_6$ in EC/EMC (3/7 in wt) + 10% FEC). The cell retains 78% capacity after 400 cycles with a stabilized coulombic efficiency of 99.9%. The superior stability of the porous Si-C anode can be attributed to 1) mitigated volume expansion with sealed porosity; 2) improved overall conductivity of the composite; and 3) the minimized electrolyte penetration into the porous Si.

The stability of PNNL's Si anode was also demonstrated in Si/NMC622 pouch cells using a carbonate electrolyte E1 (1.2 M $LiPF_6$ in EC-PC-EMC (1:3:6 by wt) + 1 wt% VC + 7 wt% FEC) as shown in Figure 1a. The cells are cycled between 2.0 to 4.35 volt (V) with 0.5C for discharge and 0.7C for charge. A capacity check cycle is done at every 50 cycles at 0.2C. The cell retains 88% capacity after 950 cycles.

To further improve life, PNNL researchers have developed several localized high concentration electrolytes (LHCE). These electrolytes have significantly improved cycle life of Si/$LiCoO_2$ pouch cells between 2.75 to 4.35V as shown in Figure 1b where the Si anode developed in PNNL is used. The cells can retain 80% capacity in 1000 and almost 2000 cycles using carbonate electrolyte E1 and PNNL's LHCE electrolyte, respectively.

Thus, the porous Si as created via PNNL's method has potential to enable the next generation of high-energy lithium batteries, while the LHC electrolyte provides new understanding of electrolyte functionality with Si anodes towards further potential enhancements in Si anode capability.

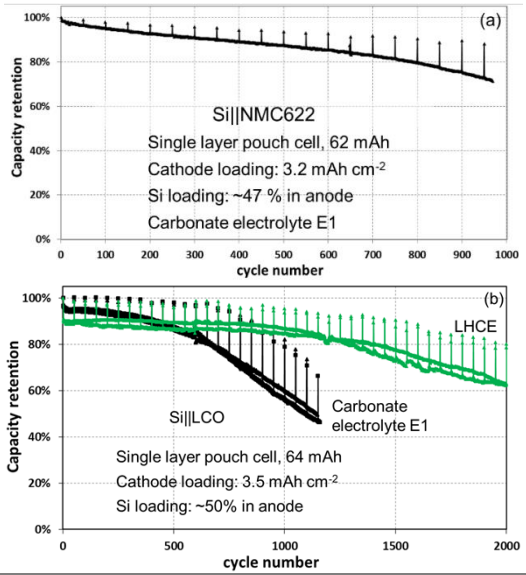

Figure 1. (a) Cycling of Si/NMC622 cells using porous Si anode and carbonate electrolytes E1. (b) Cycling stability of Si/$LiCoO_2$ cells using porous Si anode and different electrolytes.

2020 U.S. DRIVE Highlight

Synthesis of High-Performance Nickel-Rich Cathode Materials for High-Energy Batteries

Researchers identified cost-effective approaches to synthesize high-performance cathode materials for next-generation lithium-ion batteries.

Pacific Northwest National Laboratory

Nickel (Ni)-rich cathodes are one of the most promising materials for next-generation, high-energy lithium (Li)-ion batteries, but it suffers from moisture sensitivity, side reactions, and gas generation during cycling. A single crystalline, Ni-rich cathode may address the challenges present in its polycrystalline counterpart by reducing phase boundaries and materials surfaces; however, synthesis of electrochemically active Ni-rich single crystalline cathodes remains challenging. Ni-rich cathodes require lower synthesis temperatures because of their structural instability at high temperatures, opposite to the high-temperature and time-consuming calcination process needed to grow single crystals.

Researchers at Pacific Northwest National Laboratory (PNNL) recently identified two cost-competitive synthesis routes (compared to traditional single crystal synthesis methods) to prepare single crystalline $LiNi_{0.76}Mn_{0.14}Co_{0.1}O_2$ (NMC76). The route used here is a molten salt one using NaCl, the second is a solid-state approach which is currently being further developed in collaboration with Albemarle under a separate DOE project. Figure 1 displays the cycling stability of NMC76 at different cutoff voltages. All material evaluations were conducted using high mass-loading (>20 mg/cm^2) single crystals in full coin cells with a graphite anode. Between 2.7 and 4.2 volt (V) (versus graphite), single crystalline NMC76 delivers 182.3 mAh/g discharge capacity at 0.1 C and retains 86.5% of its original capacity after 200 cycles (Fig. 1A). As expected, increasing the cutoff voltage improves the capacity, but cell degradation is faster (Fig. 1B–C).

Fig. 1D–F compares the corresponding morphologies of single crystals cycled at different cutoff voltages. If charged to 4.2V (Fig. 1D), the entire single crystal is well maintained. Increasing the cutoff voltage to 4.3V results in some visible gliding lines on the crystal surfaces (Fig. 1E). When cut off at 4.4V, single crystals are "sliced" (Fig. 1F) in parallel. Small cracks were also discovered cycled between 2.7 and 4.4V. Although single crystalline NMC76 as an entire particle is still intact (Fig. 1D–F) even at high cutoff voltages, gliding is the major mechanical degradation mode. PNNL researchers have identified a critical crystal size of 3.5 μm, below which gliding and microcracking will not occur, providing clues to further improve single crystal performances in the future. This work has recently been published in Science (December 10, 2020).

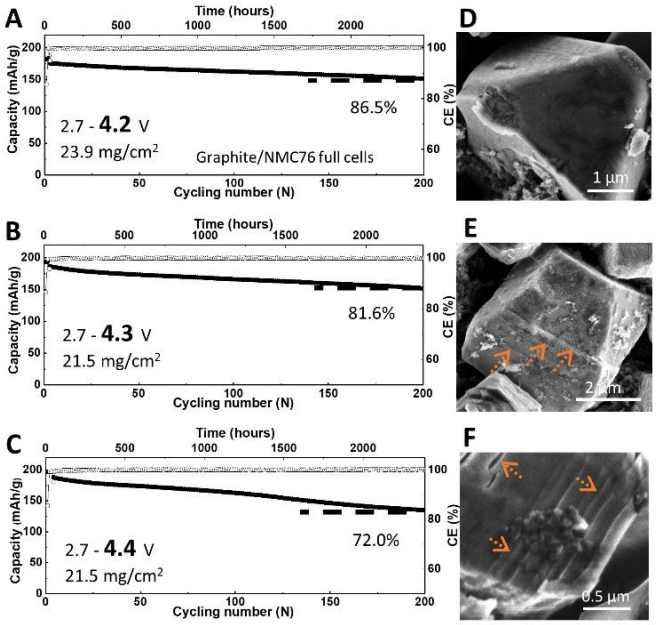

Figure 1. Cycling stability of single crystalline NMC76 in full cells between 2.7V and (A) 4.2V, (B) 4.3 V, and (C) 4.4 V vs. graphite. (D), (E), and (F) are the corresponding Scanning Electron Microscope images of the cycled single crystals in (A), (B), and (C), respectively.

2020 U.S. DRIVE Highlight

A New Electrolyte Solvent Molecule Enables Lithium Metal Batteries

A synthesized solvent molecule, FDMB, is rationally designed, and the resulting single-salt, single-solvent, low-concentration electrolyte is shown to enable anode-free pouch cells.

Stanford University and SLAC National Accelerator Laboratory

Lithium (Li) metal batteries have been identified as a next-generation battery, yet they are restrained by poor performing electrolytes. Conventional electrolytes fall short when used with Li metal anodes, let alone anode-free Li-based batteries. Previous electrolyte engineering reports improved the cycling efficiency of Li metal anodes, but have not completely addressed the following key parameters: (1) high Coulombic efficiency (CE) to minimize Li loss, including in the initial cycles; (2) use of lean electrolyte and limited-excess Li conditions for maximized specific energy; (3) high oxidative stability towards high-voltage cathodes; (4) reasonable salt concentration for cost-effectiveness; and (5) high boiling point and non-flammability for safety and processability.

This team reports a new electrolyte that shows promise to meet the above requirements (Nature Energy, 5, 526-533, 2020). Fluorinated 1,4-dimethoxybutane (FDMB, Figure 1a), is paired with 1 M lithium bis(fluorosulfonyl)imide (LiFSI) in a single-salt, single-solvent electrolyte formulation (LiFSI/FDMB) to enable stable, high energy-density Li metal batteries. The 1 M LiFSI/FDMB electrolyte reveals a high CE (~99.52%) and fast activation (Li|Cu half-cell CE ramps up to more than 99% within 5 cycles) for Li-metal anodes. The Li|NMC full cells with limited-excess Li retain 90% capacity after 420 cycles with an average CE of 99.98% (Figure 1b). Furthermore, anode-free Cu|NMC811 pouch cells achieve ~325Wh/kg whole-cell energy density, while Cu|NMC532 pouch cells realize ~80% capacity retention after 100 cycles at 20°C, which is one of the best performances among the state-of-the-art anode-free cells (Figure 1c). The 1M LiFSI/FDMB electrolyte also enables fast discharge capability in anode-free pouch cells, which magnifies its potential application in the field of premium energy storage applications (Figure 1d). Our rational design concept for new electrolyte solvents provides a promising path to viable high-energy Li metal batteries and anode-free pouch cells with high cyclability and processability and may aid in advancing understanding for more widespread and lower cost energy storage applications.

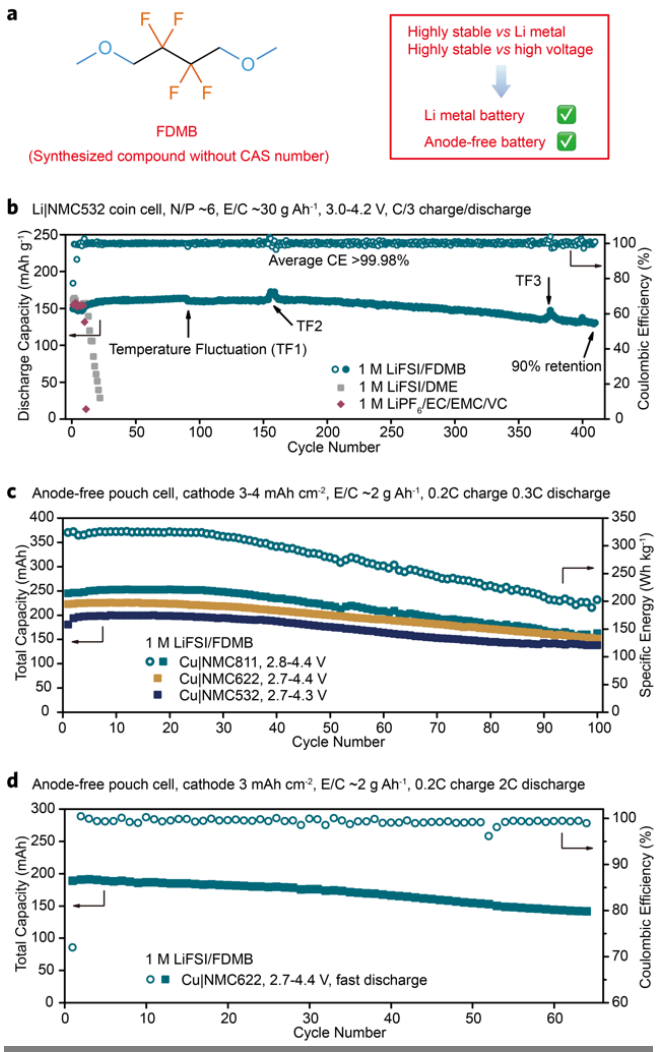

Figure 1. (a) Molecular structure of FDMB. (b-d) Cycling performance of Li metal batteries and anode-free pouch cells.

2020 U.S. DRIVE Highlight

Improved Extreme Fast Charge Tolerance in Graphite Anodes via Metal Film Surface Coating

Graphite anodes modified with nanoscale metallic films improve capacity retention of lithium-ion batteries cycled under 10-minute charge.

Stony Brook University and Brookhaven National Laboratory

The development of lithium-ion (Li-ion) batteries that can be charged in 10–15 minutes without sacrificing driving range, cost, or cycle life is critical for the increased adoption of electric vehicles. The primary technical barrier preventing repetitive extreme fast charging (XFC) of Li-ion batteries is deposition of electrochemically isolated lithium metal on the graphite anode resulting in capacity degradation and safety issues.

Researchers at Stony Brook University (SBU) and Brookhaven National Laboratory (BNL) have recently invented a new approach for suppressing lithium metal deposition on the graphite anode under XFC conditions. They deliberately modify the anodes with metallic (copper or nickel) nanoscale surface films which have high overpotentials unfavorable for Li metal nucleation (Figure 1).

In a recently published paper (https://dx.doi.org/10.1149/1945-7111/abcaba) the effectiveness of metallic surface coatings with different areal loadings at reducing capacity fade under XFC was explored. Cells with graphite electrodes with high metal film loadings exhibited an improvement (9%) in capacity retention after 500 XFC (10-minute) cycles versus uncoated anodes (Fig. 2). The metal coating did not impact the 1C discharge capacity. Li metal deposition quantified by X-ray diffraction supported these findings, with higher loading metal films exhibiting enhanced Li plating suppression compared to lower loading films. Transmission electron microscopy imaging revealed that the higher loading films have more complete coverage of the graphite surface, permitting more effective overpotential control. The results highlight the use of nanoscale surface coatings for prevention of Li plating during XFC.

Future research efforts are centered on demonstrating that the metal film coated electrodes can be fabricated using a cost-effective, scalable approach that preserves the functional benefits observed for laboratory scale fabricated films.

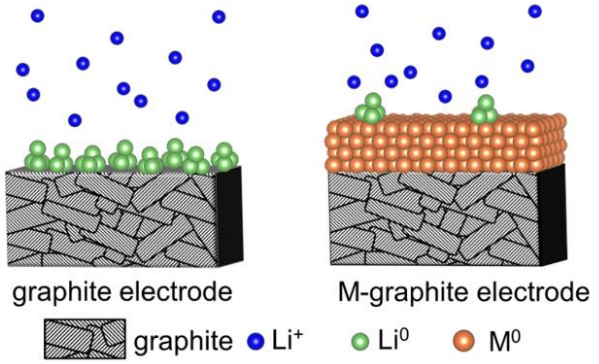

Figure 1. Schematic representation of the approach for suppressing Li metal plating during high charging current: nanoscale metallic films applied to the upper surfaces of battery anodes increase the overpotential for the Li nucleation.

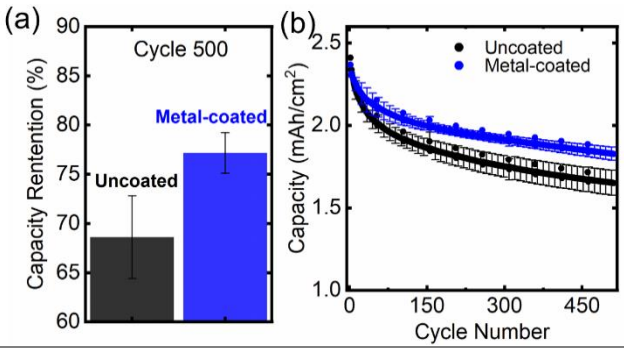

Figure 2. (a) 500 cycle capacity retention and (b) areal capacity for Li-ion pouch cells with uncoated (control) and nanoscale metal coated electrodes cycled under 10-minute charge rate, 6C constant current charge to 4.3 volt followed by a constant voltage hold for the remainder of the 10 minutes.

2020 U.S. DRIVE Highlight

A New Pathway to Higher Energy Density: Cobalt-Free Cathodes Enabled by 3D Targeted Doping

Enhancing oxygen stability in low-cobalt layered oxide cathode materials by three-dimensional targeted doping.

University of California—Irvine

As high nickel cathode cell chemistries have reached initial market penetration, a grand challenge for the field is a quest for cobalt (Co)-free layered cathodes to reduce the reliance on high-cost and toxic Co. However, it is well known that $LiNiO_2$ (LNO) has high capacity but is thermally unstable at charged state and has poor cycle life. To enhance its performance requires structure-stabilizing elements such as Co. Even though the instability of LNO seems to render its use in a commercial cathode unlikely, it shares many of the problems of currently employed NMCs that have potential to be resolved using specialized dopants or electrolytes targeting the instability of the cathode/electrolyte interfaces.

The Low/No-cobalt project led by the University of California (UC)—Irvine with team members from Virginia Tech, UC Berkeley, and Pacific Northwest National Laboratory have developed a three-dimensional (3D) targeted doping technology that combines surface and bulk doping with nanometer precision. The team used computationally selected surface dopants. They introduced theory-rationalized bulk dopants to the interior of the particles to further enhance oxygen stability and inhibit deleterious phase transition in Co-free oxides under high-voltage and deep-discharging operating conditions.

As shown in Figure 1b, the team has enabled three-dimensional targeted doping on the surfaces of the cathode particle with nanometer precision. In the meantime, the layered atomic structures are preserved with nearly no secondary phase on the surfaces. More importantly, the surface/bulk titanium/magnesium doping significantly improve the cycling performance of the Co-free and extremely high-nickel chemistry ($LiNi_{0.96}Ti_{0.02}Mg_{0.02}O_2$), reaching a cycle life of 400 cycles (2.5–4.4 volt vs. Li).

Future work will include full cell cycle life tests and evaluating the cathode particles for improved resilience to cracking or other damage.

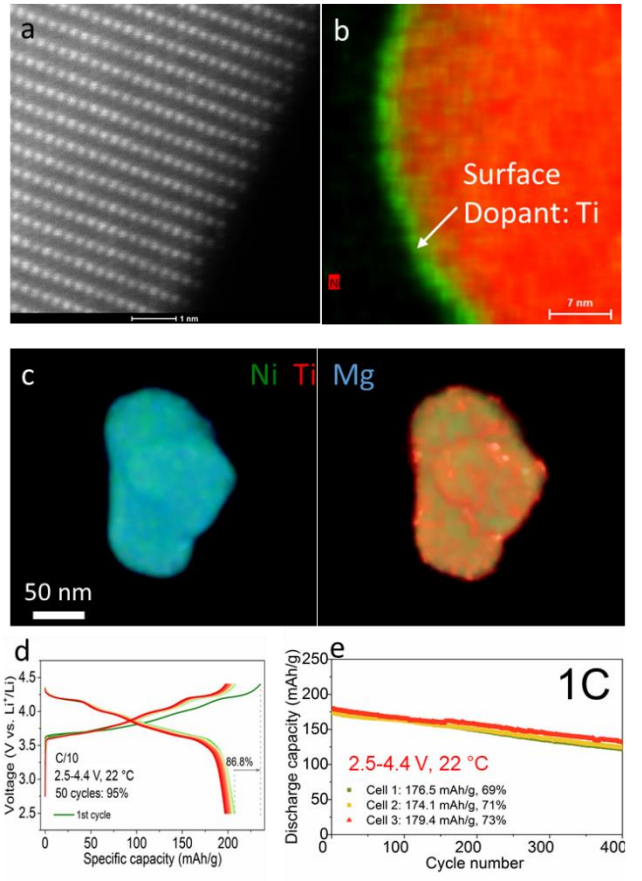

Figure 1. (a-b) Structure and chemical imaging of the Co-free cathode particles. (c) 3D nano-electron-tomography imaging of the dopant distribution. (d-e) The electrochemical performance of the Co-free cathode materials.

2020 U.S. DRIVE Highlight

Laser-Patterned Electrodes for Enhanced Fast Charge Capability

Researchers have demonstrated efficient and long-term fast-charge cycling of lithium-ion batteries enabled by laser-patterned electrodes, using commercially relevant multilayer pouch cells.

University of Michigan and Sandia National Laboratories

Enabling lithium (Li)-ion batteries with high energy and fast-charging capability would accelerate public acceptance of electric vehicles. However, in order to achieve high energy, thick electrodes are often used, which hinders the ability to fast-charge, leading to a tradeoff between power and energy density.

Researchers at the University of Michigan have developed a laser patterning process to precisely form pore channels into graphite anodes. This process results in a highly ordered laser-patterned electrode (HOLE) architecture consisting of arrays of vertical channels through the electrode thickness, as shown in Fig 1. The pore channels facilitate rapid transport of Li-ions into the bulk electrode. As a result of the improved transport, the concentration of Li-ions throughout the electrode is more homogeneous, leading to a higher accessible capacity and lower propensity for Li plating during extreme fast-charging (XFC).

The HOLE design was applied on industrially relevant, >2 Ah pouch cells (>3 mAh/cm^2 graphite anodes) and demonstrated improved capacity retention during fast-charge cycling, compared to conventional electrodes. After 600 fast-charge cycles, the capacity retention of the HOLE cells is 91% at 4C (15-min) and 86% at 6C (10-min) charge rates, Fig 2. This is compared to 69% and 59% retention for unpatterned electrodes under the same conditions (not shown). Moreover, the HOLE design allows for cells to access more than 90% of the total cell capacity during fast charging. The design results in less than 10% reduction in electrode capacity, which can be compensated for by starting with a higher loading anode. The improved charging performance has been further validated by Sandia National Laboratories.

The laser patterning approach is compatible with current Li-ion battery manufacturing. The Michigan team is currently working toward scale-up and integration of their HOLE technology into roll-to-roll manufacturing lines. The HOLE architecture can enable electric-vehicle-scale batteries that can maintain long range, while simultaneously reducing charging time.

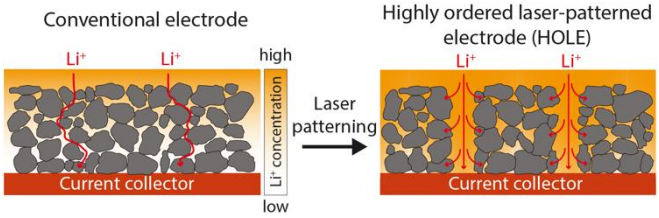

Figure 1. Schematic illustration of the conventional electrode and highly ordered laser-patterned electrode (HOLE) design.

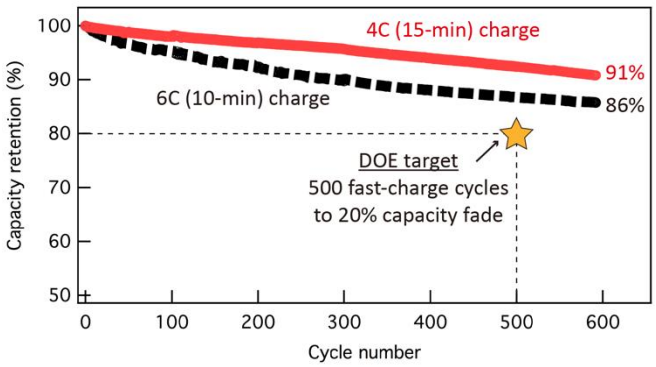

Figure 2. Capacity retention of 2.2 Ah HOLE pouch cells during long-term fast-charge cycling at 4C (15-min) and 6C (10-min) charge rates. The DOE target is labeled in the figure as a reference. Figs. 1 and 2 reproduced with permission from K.-H. Chen et al., *Journal of Power Sources* 471, 228475 (2020).

Fuel Cells

2020 U.S. DRIVE Highlight

New Catalyst-Support Materials to Improve Durability

Niobium oxide incorporated on carbon supports via physical vapor deposition method led to high durability catalyst material.

Ford Motor Company

Improving the activity and durability of the catalyst is a high R&D priority for widespread fuel cell adoption. State-of-the-art fuel cells use platinum (Pt)-alloy nanoparticles dispersed on carbon black supports as a cathode catalyst. However, the alloying element can leach out and the carbon support is susceptible to corrosion, leading to fuel cell degradation. Ford has developed new Pt/NbOx/C catalysts that shows high activity and unusually high stability.

Fuel cell catalysts are commonly prepared by wet synthesis using liquid solvents and heat treatment. This limits some elements and structures to be explored due to the interaction with the solvent. In this project, physical vapor deposition (PVD) was used to deposit both Pt and niobium oxide (NbOx) on carbon black support. This allows a more precise control of the NbOx stoichiometry, which is critical because NbOx has several crystalline variants, some of which are unstable or electrical insulated. Cost analysis done by Strategic Analysis suggested that Pt/NbOx/C catalysts made via PVD process can be economically viable.

The team demonstrated Pt/NbOx/C catalysts with mass activity as high as 0.39 A/mg_{PGM}. While this is slightly lower than the U.S. Department of Energy's (DOE) target of 0.44 A/mg_{PGM}, it is higher than that of conventional pure Pt catalysts. What is surprising is the improved stability of this catalyst. The catalyst satisfied both the catalyst- and the support-stability tests set by DOE, showing only 14% and 7% mass activity losses, respectively (versus 40% targets, Figure 1 right). The result from the support stability test is particularly impressive for a dispersed catalyst containing carbon.

The project further investigated the origin of the improvement in activity and stability using 3D electron microscopy and synchrotron X-ray absorption spectroscopy. They found that Pt nanoparticles form a connected network adjacent to NbOx clusters. Surprisingly, no Pt-Nb electronic interaction was confirmed. On the other hand, electron transfer from Pt to O was observed for a wide range of potential. This explains why Pt is tightly anchored to NbOx and its improved stability. It was also proposed that the electron transfer from Pt to O of NbOx suppresses the electron transfer from Pt to ORR intermediates, weakening the Pt-O bonding energy, and increases its catalytic activity.

The learnings from this project may lead to development of a new family of high activity durable fuel cell catalysts. Future works include scaling up for validation in a larger cell, improving the catalyst dispersion, and exploring the catalyst composition and alloying element to further improve its performance.

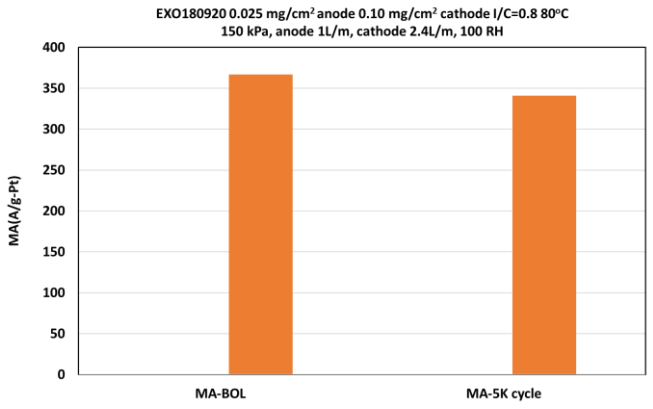

Figure 1. Pt/NbOx/C catalyst showed only 7% catalytic activity loss after support stability test, surpassing DOE target of less than 40% loss.

2020 U.S. DRIVE Highlight

Operating Conditions to Enhance Membrane Electrode Assembly Durability Identified

Knowledge of degradation mechanisms provides additional insight towards meeting durability target.

General Motors

Durability and performance are the major barriers for automotive fuel cell commercialization. In this project led by General Motors (GM), the objective was to enhance the durability of state-of-the-art membrane electrode assemblies (MEA's) through optimization of operating conditions, instead of material innovation. For electrode durability, the team pursued a design of experiments to map the impacts of temperature, relative humidity (RH), and upper voltage on the degradation behaviors in voltage cycling. The team developed a statistical model with predictive equations for electrochemical active surface and power losses. Furthermore, Argonne National Laboratory's (ANL) predictive model was refined with the voltage cycling data from this project, and then used to identify the desired operating conditions that could prolong the electrode durability to 5000 h and 8000 h in drive cycles. For membrane durability, the team gained fundamental knowledge on migration of chemical stabilizer cerium and synergistic effects of mechanical and chemical degradations, which is expected to contribute to the development of a unified predictive degradation model.

Through the design of experiments, statistical analysis, and modeling, GM was able to map the impact of operating conditions and derive a benign operating window to prolong the lifetime. Figure 1, one can see different operating windows for RH, temperature, and upper voltage to retain less than 20% electrochemical area (ECA) loss at end-of-life (EOL) after 60 K voltage cycles. Together with ANL's model, the team was able to demonstrate achieving 5000 h and 8000 h electrode life in drive cycle by mitigating upper voltage limit, reducing RH, etc.

Comprehensive cerium transport measurement and modeling has provided insights on the membrane degradation mechanism, a key trend being cerium depletion at the cathode outlet where RH cycling is dominant. Accumulating cerium in the non-active area has been observed experimentally and captured by modeling. Furthermore, because both mechanical and chemical stresses can accelerate membrane degradation, ex situ experiments were conducted to understand the interaction between mechanical stress and fluoride emission rate (FER, an indicator of chemical degradation), as shown in Figure 2.

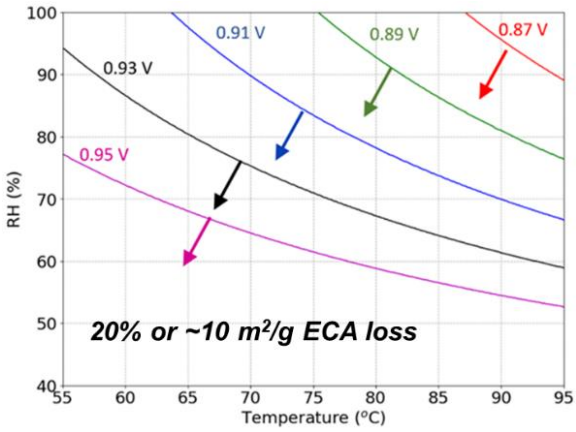

Figure 1. Operating window to retain less than 20% ECA loss or 10% voltage loss at EOL, obtained from modeling together with design of experiment data.

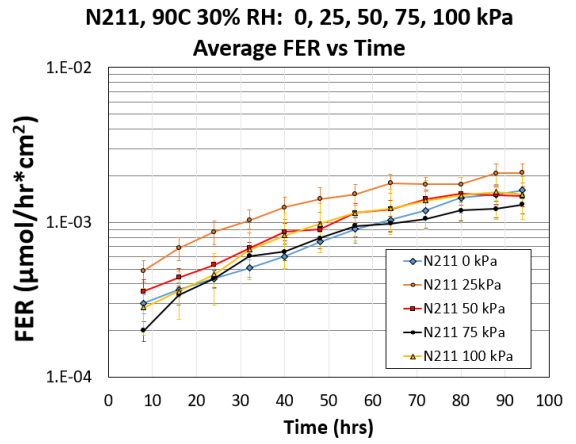

Figure 2. Fluoride emission rates under differential pressures.

2020 U.S. DRIVE Highlight

Ordered Intermetallic Nanoparticle Catalysts Demonstrate High Activity and Improved Durability

Ordered-intermetallic catalysts demonstrate improved durability in a membrane electrode assembly while providing the performance benefits of alloys, meeting catalyst activity and durability targets.

Los Alamos National Laboratory

The activity of platinum (Pt) catalysts can be improved by alloying Pt with other metals. Alloys with nickel (Ni) or cobalt (Co) show improved activity and have been developed into commercial catalysts. However, these alloys tend to have lower durability than pure Pt catalysts, as the Ni or Co leach from the alloy catalyst particle during fuel cell operation. Los Alamos National Laboratory (LANL) has developed alloy catalysts that maintain high activity and reduce the dissolution of the non-Pt metal. The key to the improved durability is obtaining an ordered structure in the alloy particle, as illustrated in Figure 1.

Previous work in this project had demonstrated the durability of these ordered nanoparticle catalysts. In this past year, LANL has improved their understanding of how to form the ordered structures and how the structure improves durability. The ordered intermetallics have reduced areas of high Co or Ni content. Density functional theory calculations indicate these high-Co content areas reduce the barrier for Co diffusion, making leaching of the Co easier.

Forming a Pt skin on the surface of the ordered intermetallic particles further reduces Co leaching. LANL has investigated the impact of the Pt skin thickness on both durability and performance. As shown in Figure 2, the ordered-intermetallic PtCo with thick Pt shell layers (more than 0.5 nm) had higher durability and higher end-of-life (EOL) performance than that with thin Pt shells (less than 0.5 nm), but slightly lower beginning-of-life (BOL) performance. The thicker Pt shell reduced the performance loss at 0.8 A/cm² after cycling from 35 mV for the thin shell catalysts to 19 mV for the thick shell catalyst, meeting the U.S. Department of Energy's (DOE) target (more than 30 mV). LANL has also investigated the impacts of catalyst particle size on the activity and durability of these intermetallics. Decreasing the particle size from 4-5 nm to 3-4 nm increased catalyst mass activity but resulted in reduced durability. The literature indicates smaller PtCo particles have poor ordering. LANL has discovered that adding zinc to form a ternary system improves ordering, which may lead to smaller, more active durable catalysts in the future.

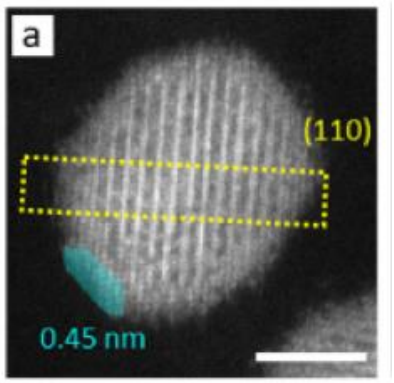

Figure 1. STEM micrograph of an ordered intermetallic PtCo particle with a 0.45 nm Pt shell.

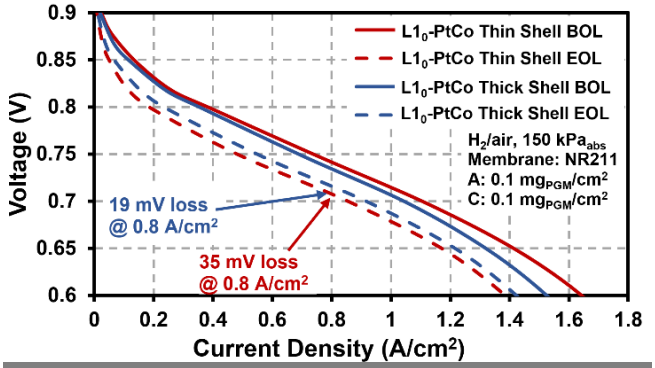

Figure 2. LANL has deposited the binary PtCo catalysts on carbon supports and integrated these catalysts into membrane electrode assemblies that meet DOE targets for mass activity (>0.44 A/mg PGM), catalyst durability (40% loss in mass activity, 30 mV loss in performance at 0.8 A/cm²), and performance (>1 W/cm²).

2020 U.S. DRIVE Highlight

Fuel Cell Modeling and Cost Analysis Highlight Research Opportunities for Heavy-Duty Vehicles

Detailed cost models provide documented public reference for annual assessment of progress towards the U.S. Department of Energy's Hydrogen and Fuel Cell Technologies Office goals.

Strategic Analysis Incorporated

Fuel cell cost analysis is critical for demonstrating the significant progress that has been made through research and development activities and in identifying potential areas of R&D focus for cost reduction. It also provides the fuel cell community with a referenceable standard widely utilized in further analyses. In the past year, Strategic Analysis, Inc. (SA) applied their fuel cell system cost analyses to medium-duty and heavy-duty (MD/HD) vehicle applications, which are rapidly becoming the primary application focus of numerous fuel cell developers and original equipment manufacturers. This study has independently estimated the cost of 2025 HD vehicle fuel cell systems at high volume production (100,000 units/yr) at $112/kW, with the U.S. Department of Energy's (DOE) ultimate target set at $60/kW. A total cost of ownership (TCO) study of Class 8 long-haul fuel cell truck suggested a ~$1.58/mi cost, ~25% higher than benchmark diesel, while providing a green solution.

SA developed their realistic automotive fuel cell power plant system cost model in collaboration with detailed performance and durability fuel cell modeling from Argonne National Laboratory (ANL), continually updated balance-of-plant data and feedback from component developers, and recent results from DOE Hydrogen and Fuel Cell Technologies Office projects. SA derives their own manufacturing process assumptions based on Design for Manufacture and Assembly techniques, and validates their assumptions with extensive industry interaction, peer review, and U.S. DRIVE Fuel Cell Technical Team Reviews.

SA applied their cost modeling analysis to identify low cost solutions applicable to the specific requirements of MD/HD applications (primarily greater durability and lifetime). The team performed a comprehensive review of durability-enhancing options and assessed cost impact. Results assist the DOE and community in driving R&D targets such as ranges for recommended precious metal catalyst loadings (higher than light-duty vehicles [LDV]), operating temperature (below LDV for enhanced durability), cell voltage optimization, fuel cell stack power density, and FC/battery hybridization. This analysis provides insights that will help guide the direction of the new Million Mile Fuel Cell Truck (M^2FCT) consortium.

The team performed a detailed TCO study for a Class 8 long-haul HD fuel cell application, finding that the TCO is most sensitive to truck ownership life and fuel cost. System efficiency has also been identified as a significant driver of overall cost. Such a model can be exercised in future studies to further optimize fuel cell design and operation for the more relevant TCO rather than just initial system cost. Studies may include refinement of target durability enabler assessments, maximum operating temperature, and catalyst loadings.

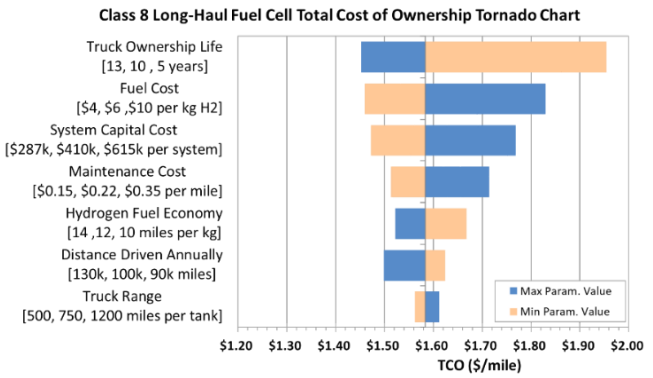

Figure 1. Class 8 long-haul truck total cost of ownership tornado chart shows hydrogen cost and truck life (durability) as key drivers.

Materials

2020 U.S. DRIVE Highlight

Corrosion Protection of Dissimilar Material and Joining for Next-Generation Lightweight Vehicles

Evaluation of corrosion behavior of a multi-material joining technology that leverages the existing resistance spot welding automotive infrastructure.

Arconic Technology Center

The Arconic Technology Center is working with Honda R&D Americas, LLC and the Ohio State University (OSU) to evaluate the corrosion performance and demonstrate the production worthiness of the Resistance Spot Riveting (RSR™) process. RSR is a new technology being developed by Howmet Fastening Systems (formerly Arconic, Inc.) that employs a fastener that is installed using conventional resistance spot welding equipment to produce multi-material joints.

The goal of the 3-year project is to demonstrate the use of RSR to join aluminum (Al) to steel and Al to carbon fiber composites on a prototype scale. Deployment of this technology would help the automotive industry achieve an additional 10%-20% weight reduction over high strength steels. These weight-savings to the body in white generally translates to 2.5%-5% of overall vehicle curb weight. The resulting total weight-savings could provide a 1.5% to 3% total improvement in fuel efficiency for vehicles that incorporate RSR for multi-material joining.

The RSR technology addresses several production barriers to achieving the U.S. Department of Energy's fuel efficiency targets including eliminating the need of additional capital for new joining technologies, and the flexibility to process conventional steel and multi-material structures with the same equipment. Additionally, the trend towards ultra-high strength steels limits the availability of conventional joining technologies that can effectively process these multi-material combinations. In order to accomplish these goals, the following program milestones were developed by the team:

- Develop RSR process parameters, producing multi-material joints for mechanical testing and corrosion assessments.
- Conduct corrosion evaluation and choose a corrosion mitigation strategy.
- Develop a production ready feed system and mount to a robotic system to simulate production conditions.
- Produce demonstration assemblies for testing and evaluation.

The fourth year of this project focused on completing the corrosion studies at OSU and Honda. The last program milestone, fabrication and testing of the demonstration articles, is targeted for completion in early 2021. Fabrication using the RSR robotic assembly cell was planned in two steps. Initial assemblies would be used to establish the design and verify the mechanical performance against Honda's predicted simulations. Changes would then be incorporated into the final demonstration pieces targeted to be tested by testing at Honda in January 2021. A photo of the initial demonstrator is shown in Figure 1.

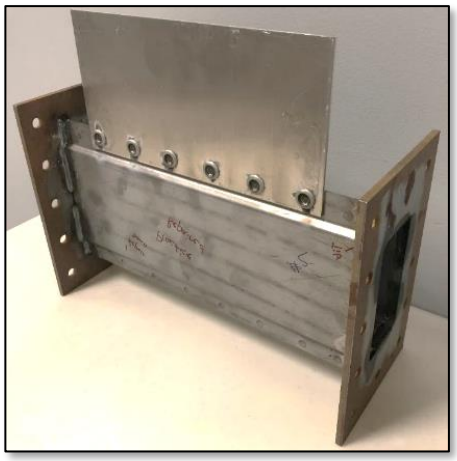

Figure 1. Assembled demonstrator prior to mechanical testing. Source: Honda

2020 U.S. DRIVE Highlight

Low-Temperature Carbonization/Close Proximity Electromagnetic Carbonization

Development of a new process for low temperature carbonization stage of the conversion of carbon fiber using an electromagnetic power source.

Oak Ridge National Laboratory & 4XTechnologies

The goal of the close proximity electromagnetic carbonization (CPEC) project is to develop a novel carbonization technique to replace existing conventional low-temperature carbonization (LTC) equipment in the carbon fiber (CF) industry. It is a joint development project funded by the U.S. Department of Energy, with research carried out by Oak Ridge National Laboratory (ORNL) (technical lead) and 4XTechnologies, LLC (formerly RMX Technologies). In 2017, the team developed a first prototype that successfully carbonized one single continuous tow at LTC within less than a minute of residence time. The tensile strength and the modulus of the CF (achieved after HTC) were in the 300-350 ksi and 22.5-25.5 Msi ranges, respectively. Subsequent effort was dedicated to scaling up this process (multiple continuous tows) and demonstrating its advantages regarding costs, energy consumption, or other benefits. At the end of 2019, a subsystem failed, prompting reevaluation of the system design. Two new designs were investigated and the one with the largest modification was implemented.

With the new applicator, the mechanical properties of material were measurably improved. Almost all fiber entirely converted (after HTC) surpassed 500 ksi for the tensile strength and reached a modulus of 30 Msi while keeping a residence time significantly shorter than 1 minute at LTC (Figure 1). With this process, the span of residence time explored at LTC showed low effects on the final product (CF). Finally, density measurements indicated that this setup processes the tows unevenly. Based on results after HTC, this had minimal impact on the mechanical properties of the final CF. Compared to the thriftiest benchmark available regarding energy efficiency (1.74 kWh/lb), the measurements indicate that energy reduction in the range of 40%-50% is possible with the existing setup under the following conditions: throughput must be maximized, and control volume must be limited to the usable energy (e.g., the electromagnetic energy). Further development will be needed to make the whole system energy profitable.

Future work will be dedicated to the application of similar technology to the HTC process to enable the targeted energy savings using the process in both the LTC and HTC process steps.

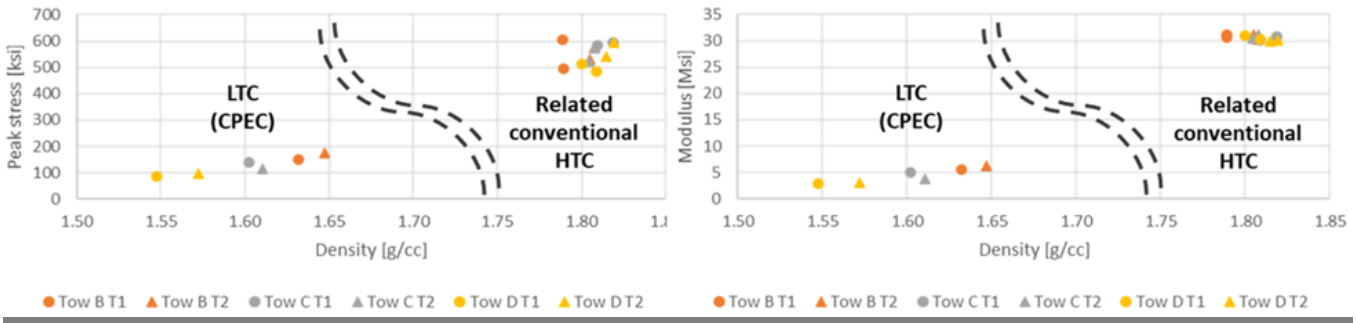

Figure 1. Mechanical properties of three from a continuous run of four simultaneous tows. Two residence times were tested with CPEC: T1 < T2 < 1min. Also, two conditions were tested HTC condition. Tow A was not characterized. Process was not optimized. (Left) Plot "Peak stress vs. Density" and (Right) Plot "Modulus vs. Density."

2020 U.S. DRIVE Highlight

Self-Sensing Fiber Reinforced Composites

Fiber coating method to enhance the sensing and mechanical performance of multifunctional composites for vehicle lightweighting.

Oak Ridge National Laboratory

Researchers at Oak Ridge National Laboratory (ORNL) developed a patent-pending process for integrating nanoparticles onto the surface of carbon fiber. The goal was to enhance both the sensing and mechanical performance of the multifunctional composites. The obvious benefit of increased mechanical performance is weight reduction to meet design specifications. Integrated self-sensing further reduces the weight by negating the need to attach sensors to the composite for structural health monitoring.

Researchers selected titanium dioxide (TiO_2) nanoparticles for their piezoresistive behavior, which exhibits varying electrical resistance in response to applied force. These nanoparticles were embedded into the polymer sizing that typically coats carbon fiber. The sizing acted as a carrier matrix to adhere the nanoparticles to the fiber surface. The result was a facile and rapid process for commercial adoption and provided excellent control of the concentration and dispersion of nanoparticles on the fiber surface.

For mechanical performance evaluation, unidirectional composites were fabricated and tested using the short beam shear method, which quantifies the apparent interlaminar shear strength. An optimum range of 0.5-1.5wt% nanoparticles was found to give the best performance with up to a 14.7% increase in interlaminar shear strength.

Sensing performance was characterized by measuring electrical resistance of a cantilever beam subjected to varying strain levels. The resulting value is called the gauge factor, which is the electrical resistance change divided by the strain applied. A higher gauge factor represents better sensitivity. Overall, the 2.5 wt% nanoparticle composite showed the best sensing performance with a 187% increase in gauge factor compared to the baseline composite.

Figure 1 summarizes the mechanical and sensing performance of the composites. The upper right, yellow quadrant highlights the composites that saw simultaneous improvements in both properties as compared to the baseline composite. Overall, the 1 wt% nanoparticle composite performed best with improvements of 14.7% and 172% in interlaminar shear strength and gauge factor, respectively.

ORNL worked with Dronesat, LLC to design structural health monitoring composites for implementation into Dronesat's prototype air transport vehicles. Further work is being conducted with Dronesat for in-field composite testing.

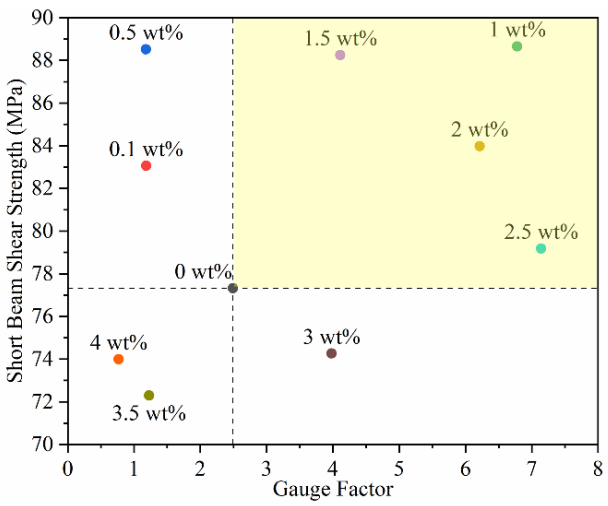

Figure 1. Plot comparing the mechanical and sensing performance of the composites with different concentrations of TiO_2 nanoparticles

2020 U.S. DRIVE Highlight

Ultrasonic Spot Welding of Magnesium to High-Strength Steel Sheets

A solid-state joining technology to join lightweight dissimilar materials that are unweldable by conventional fusion welding methods.

Oak Ridge National Laboratory

With increasing demand of lightweight materials in automobiles to reduce fuel consumption and greenhouse gas emissions, magnesium (Mg) alloys have received much attention due to their low density and high specific strength. However, joining Mg alloys with steel structures is challenging. This is because the physical and chemical properties of these two materials are very different. The melting point of Mg is 650°C versus steel or iron (Fe) at approximately 1500°C. Mg and Fe are immiscible and no intermetallic compounds are formed in the Mg/Fe system. The solubility between them is very low. Thus, although bonding of coated steel with Mg alloy have been possible via brazing, Mg to uncoated steel is considered unweldable by conventional fusion welding methods.

Ultrasonic spot welding (USW) technology provides a potential option to overcome the technical barriers preventing robust and reliable joining of Mg to steel. During USW processes, the ultrasonic transducer delivers a moderate clamping force and a high-frequency interfacial vibration into the joint interface. The welding heat is mainly generated through interfacial friction, but the temperature rise is generally not sufficient to melt the materials. Instead, the high temperature and pressure at the interface induce a rapid diffusion between the substrates to form the joint.

Figure 1(a) shows the cross-section of a USW joint made with uncoated DP590 steel and AZ31B Mg alloy (3% aluminum [Al]). Figure 1(b) presents the chemical analysis across the joint interface in the center region. The high concentration of Al at the joint interface suggests the presence of Al-Fe intermetallic compounds that is critical to joint formation. Lap shear tensile testing in Figure 2 shows a peak load of approximately 5 kN achieved.

This research demonstrated the feasibility and obtains the fundamental understanding of the weldability of USW method for joining Mg-steel dissimilar metal pairs. Next steps will focus on evaluating the structural responses during the USW process and its influence on fabrication of component level structures.

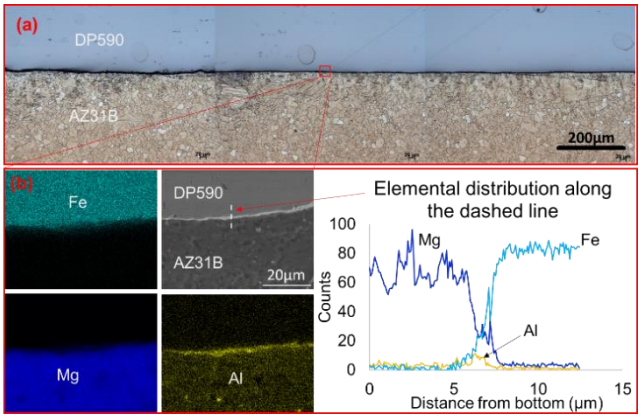

Figure 1. (a) Cross-section of a Mg-steel USW joint, (b) element distributions across the joint interface.

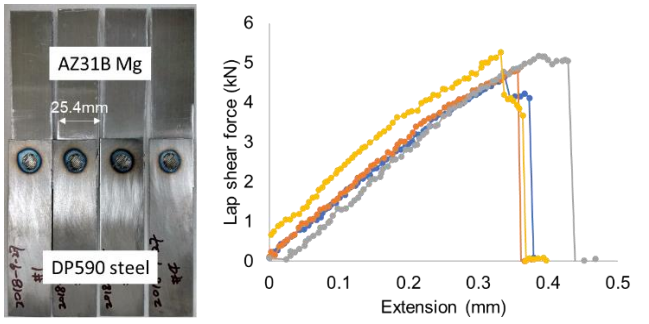

Figure 2. Lap shear coupons and lap shear tensile load versus extension curves.

2020 U.S. DRIVE Highlight

Low-Cost Aluminum and Magnesium Extrusions

Development of Shear-Assisted Processing and Extrusion to achieve improved mechanical properties using a lower cost feedstock material.

Pacific Northwest National Laboratory and Magna Collaboration

As aluminum and eventually magnesium extrusions begin to displace steel for fabricating automotive components, the impact towards lightweighting can range from a 25% to 45% weight reduction, thereby enabling greater vehicle fuel efficiency. However, this potential weight savings comes at a price and new processing methods are needed to minimize that cost. To this end, Pacific Northwest National Laboratory (PNNL) and Tier 1 supplier Magna International are co-developing Shear-Assisted Processing and Extrusion (ShAPE™) to lower the cost of aluminum and magnesium extrusions.

ShAPE is an emerging extrusion technology where feedstock material is translated into a rotating die, resulting in heat generation due to friction and severe deformation of the material. The heat helps to reduce the forces required for extruding the material and also reduces energy requirements. The combined effect of axial force and rotational shear promotes refinement of the metal grain structure and achieves better uniformity. These novel metal structures enabled by ShAPE led to improvements in material performance that result in more effective use of lightweight metals at a cost savings.

For this project, AA6063 tubing with a 12 mm diameter and 1–2 mm wall thickness (see Figure 1) was extruded at rates that are competitive with current commercial manufacturing. In other instances, ShAPE has achieved manufacturing rates over 5x that achievable by other processes. With ShAPE, the energy and cost associated with preparing the billet for extrusion and pre-heating are eliminated, and the ability to use a high percentage of secondary aluminum further reduces embedded energy and cost. The as-extruded aluminum tube responded well to aging; it had a T5 temper exceeding the ASTM standard tensile strength for the higher T6 temper, thus avoiding the cost and energy associated with post-extrusion T6 solution heat treatment and quenching steps. This represents a potential for significant overall cost and energy reduction for aluminum extrusion.

AA6063	UTS (MPa)	YS (MPa)	Elongation (%)
ShAPE™ (T5)	233	198	11
ASTM 02.02 (T6)	205	170	8

For magnesium alloys, the ShAPE process enables control of crystallographic alignment, which has been shown to virtually eliminate anisotropy, thereby bringing energy absorption of non-rare-earth ZK60-T5 on par with AA6061-T6. This project is now moving toward non-circular profiles with the goal of manufacturing multi-wall extrusions that have non-circular profiles.

The current research activity is associated with a Cooperative Research and Development Agreement through the LightMAT consortium, funded by the U.S. Department of Energy's Vehicle Technologies Office. In 2019, Magna executed a research license and option agreement, associated with the intellectual property developed by PNNL for specific fields of use. In October 2020, PNNL researchers were awarded an R&D100 award for ShAPE.

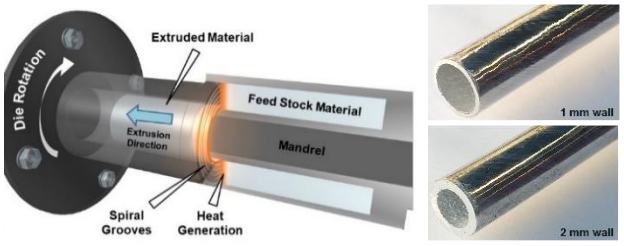

Figure 1. Cross section of the ShAPE™ tooling/process (left). AA6063 tubing with a 12 mm diameter and 1–2 mm wall thickness (right).

2020 U.S. DRIVE Highlight

Low-Cost Corrosion Protection for Magnesium

Development of a non-coating-based surface modification technique for corrosion protection in magnesium alloy sheet metal.

Pacific Northwest National Laboratory

Magnesium (Mg) is 30% less dense than aluminum (Al) but unlike Al alloys, Mg alloys have poor corrosion resistance, especially in chloride-containing environments such as those encountered in winter driving on salted roads. Because Mg is highly anodic, dissimilar Mg-based joints are susceptible to galvanic corrosion. Magnesium is one of the most promising lightweighting materials for applications in a car body and chassis, according to the U.S. Department of Energy and its partners in the automotive industry. Hence, the development of cost-effective and durable protective coatings has been identified as an important research need to help meet vehicle efficiency targets for future vehicles.

Pacific Northwest National Laboratory (PNNL) researchers are working to develop low-cost techniques to protect Mg from corrosion. Although commercial corrosion protection methods exist, they are generally expensive and involve the use of multiple chemical baths that may also have serious environmental impacts. As a result, the use of Mg sheet metal in high-volume automotive applications is still limited, and the development of corrosion protection techniques is an active area of research. To address these challenges, the team is focused on:

- Using laser surface processing (LSP) to locally modify the surface microstructure of AZ31B Mg alloy sheet metal for greater corrosion resistance relative to unprocessed sheet.
- Conducting electrochemical testing using ASTM B117 and advanced analytical techniques to correlate LSP Mg sheet corrosion behavior to its microstructure features.
- Exploring alternate techniques for producing coatings for corrosion protection without the use of harsh chemicals.

Initial ASTM B117 test results show promising corrosion protection effects of LSP on AZ31B; an order of magnitude lower corrosion product is formed relative to unprocessed sheet. Subsequent electrochemical testing also shows improved protection capability that confirms the performance of the LSP technique. By examining LSP samples via electron microscopy and other advanced techniques, PNNL researchers observed an outer ~0.5 μm thick mixed-metal (Mg, Al) oxide-hydroxide layer atop a dense, ~20 nm thick Al-rich oxide layer Figure 1). In addition, Al-Mn intermetallic particles seemed to be refined in the near-surface region as well. The combination of these features is believed to create a protective barrier and reduce the tendency for localized micro-galvanic corrosion effects, all of which result in greater corrosion resistance. The team is now exploring the potential of hydro-thermal techniques to create corrosion protection coatings.

If successful, this research will lead to lower-cost and chemically benign methods for corrosion protection of automotive Mg alloys.

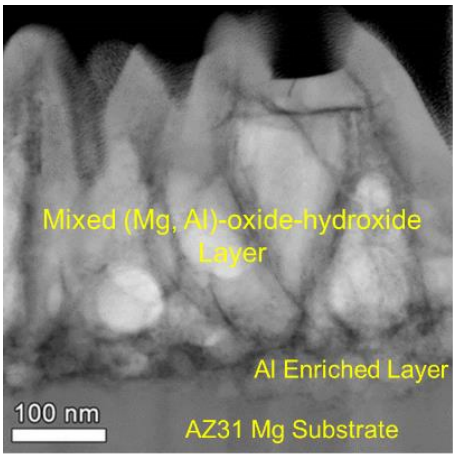

Figure. 1. A high-magnification electron-microscopy image of the surface film in a LSP Mg AZ31B sheet sample.

2020 U.S. DRIVE Highlight

Room-Temperature Stamping of High-Strength Aluminum Alloys

Novel processing approaches enable lightweight structural components made of high-strength aluminum alloys.

Pacific Northwest National Laboratory

Researchers at Pacific Northwest National Laboratory are working to overcome challenges related to stamping high-strength aluminum (Al) sheets at room temperature to form them into highly complex automotive structural components. Based on discussions with original equipment manufacturers and Tier-I industry partners, the team selected a door side-impact beam currently fabricated in steel as a demonstration component that, if stamped out of high-strength AA7075 Al alloy, would help meet the U.S. Department of Energy's (DOE's) targets for 2025: A 25% glider mass reduction relative to a comparable vehicle manufactured in 2012, and a cost penalty of no more than $5 per pound of weight saved.

Two significant manufacturing challenges are to stamp the beam at room temperature (i.e., both the sheet and the dies) without cracking, and once stamped, confirm the beam does not require artificial aging to strengthen it. These two challenges exist because alternate approaches, such as hot-stamping (to achieve the beam shape) and artificial aging (to strengthen the beam), are not cost-effective for the high-volume automotive industry. These challenges are addressed by developing a fundamental understanding of precipitation hardening kinetics. The models produced indicated the existence of more formable tempers of AA7075. The benefit of this approach has been demonstrated on commercially acquired and stamped sheet metal.

The stamped AA7075 beam (Figure 1) is approximately 38% lighter, looks identical to the baseline steel beam, and has the same dimensional tolerance. Visual examination of the Al beam does not reveal any apparent surface defects, necks, or cracks to the naked eye, indicating that the first challenge of formability has been met.

The macro-hardness was mapped across the as-stamped Al at multiple locations. Overall, about 250 hardness measurements were made of multiple beams and the average hardness was >90% of the ASTM T6 temper specification. Small-sized tensile test coupons were cut from the flat sections of the beam, and initial stress-strain data suggested they had a strength similar to the T6 temper strength, showing near-peak strength was achieved in the stamped beam without artificial aging, indicating that the second challenge has also been met.

This work has successfully developed and demonstrated an approach to stamping structural components out of a high-strength Al alloy at room temperature. We expect this approach to be more cost-effective than hot-stamping and artificial aging of high-strength Al. If this approach is extended to other structural components to replace steel with high-strength Al, it could help the automotive industry achieve the DOE's lightweighting and cost targets.

Figure 1. A side-by-side comparison of the production steel side-impact beam and the prototype high-strength Al beam.

2020 U.S. DRIVE Highlight

Predictive Tools Development for Low-Cost Carbon Fiber for Lightweight Vehicles

Development of a computational framework for carbon fiber synthesis and experimental demonstration of carbon fiber synthesis from low-cost precursors.

University of Virginia, Pennsylvania State University, Oak Ridge National Laboratory, Solvay Composites (Cytec Materials), Oshkosh Corporation

Carbon fiber reinforced polymers are stronger and lighter than engineering-grade metal alloys, so employing them in automotive structures can greatly reduce vehicle mass, thereby increasing fuel efficiency. However, their widespread adoption has been hindered by the high cost of carbon fibers (CFs). CFs are produced by thermochemically converting a polymeric fiber, called a precursor, into a fiber of carbon. This precursor accounts for over half of the final cost of a CF. Therefore, this project focused on the development of low-cost alternative CF precursors and pursued optimization of the processing techniques for CF conversion.

The team developed and utilized an integrated computational materials engineering (ICME) framework to identify alternative CF precursors (Figure 1). Under this ICME framework, precursor candidates were analyzed with ReaxFF molecular dynamics simulations to elucidate the underlying chemical reactions driving the conversion of the material across the different stages of manufacturing. The chemical structure identified via ReaxFF was then assembled into polymer ladders and built into large-scale representations of fibers. Large-scale molecular dynamics simulations were thus capable of applying loading conditions to characterize the microstructure/property relationships of the CF. The team performed experimental characterization, including single filament tensile testing, electron microscopy, and thermogravimetric analysis, to validate the simulation predictions. This ICME framework thus formed a closed-loop system of simulation and experimental validation to evaluate multiple alternative precursors to downselect candidate precursors.

The team used key insights from multiscale molecular dynamics simulations to further enhance CF conversion techniques. Simulations unveiled the role that microstructures and molecular configuration changes play in CF mechanical properties. These newly uncovered microstructure-property relationships assisted the team in optimizing the conversion of multiple alternative CF precursors. New characterization techniques were also demonstrated, including novel fiber microstructure mapping with various microscopies. Through this ICME framework, the team demonstrated low-cost carbon fibers exceeding the U.S. DRIVE targets.

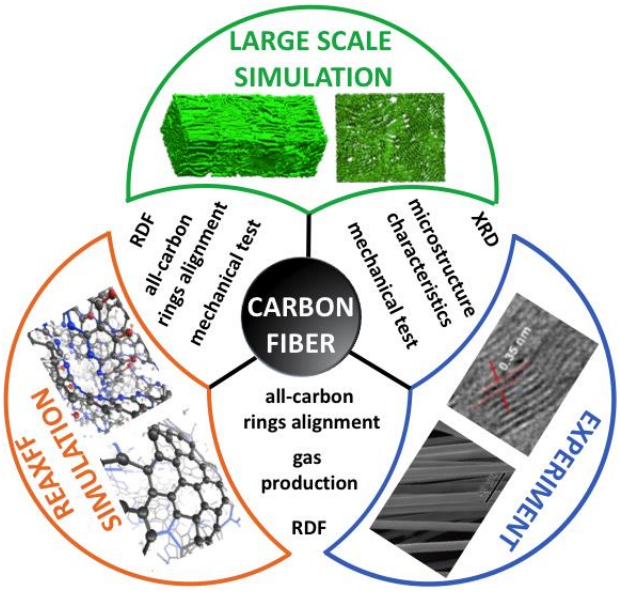

Figure 1. A graphical representation of the ICME project strategy, leveraging ReaxFF simulations to uncover the conversion of precursor materials, large-scale molecular dynamics simulations to reveal microstructural characteristics, and experimental validation of the fiber properties.

INFRASTRUCTURE AND INTEGRATION

Grid Integration

Grid Impacts of Electric Vehicle Charging at Scale are Mitigated with Smart Charge Management Solutions

Analysis of electric vehicle adoption suggests certain charging preferences could result in significant impacts to electric utility equipment that can be mitigated with smart charge controls.

National Renewable Energy Laboratory

The increasing adoption of electric vehicles (EVs) will result in significant electrical load growth in the coming decade. Driving patterns show that a vehicle's typical dwell period while parked exceeds the time required to recharge most vehicle batteries. This charging flexibility creates an opportunity to distribute charging load to facilitate a higher adoption of EVs and intermittent renewable resources. High coincident charging peaks could exceed electrical equipment capacity, resulting in the need for expensive upgrades.

The National Renewable Energy Laboratory, Sandia National Laboratories, and Idaho National Laboratory have developed models for EV load growth in Atlanta and Minneapolis. The models incorporate vehicle travel patterns, light-duty EV adoption rates, and charging preferences to assess overall energy needs. Figure 1 displays a 24-hour load profile for a primarily commercial feeder in Atlanta during a summer peak day with a regional clustering of EV adoption at 30%.

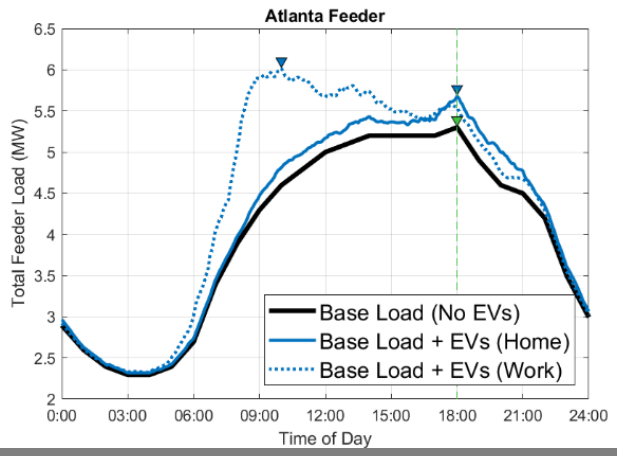

Figure 1. The EV home-dominant case increases peak load by 500 kW, whereas the work-dominant case increases energy and power needs, while shifting the peak 8 hours earlier. These differences are due to workplace charging drawing in more commercial load from nearby residential feeders.

Although charging and infrastructure preferences can shift EV profiles, a more direct approach is needed to mitigate grid impacts. The project team developed smart charge controls to mitigate impacts such as an overloaded primary circuit by shifting EV charging load within a vehicle's dwell period. The centralized control schedules EV charging to reduce the feeder peak, while another schedules a random distribution. They are compared to strategies that mimic adherence to time-of-use (TOU) rates which incentivize charging within low-cost windows as shown through either immediate or randomized start-time controls. Figure 2 displays the 24-hour EV load for a Minneapolis feeder.

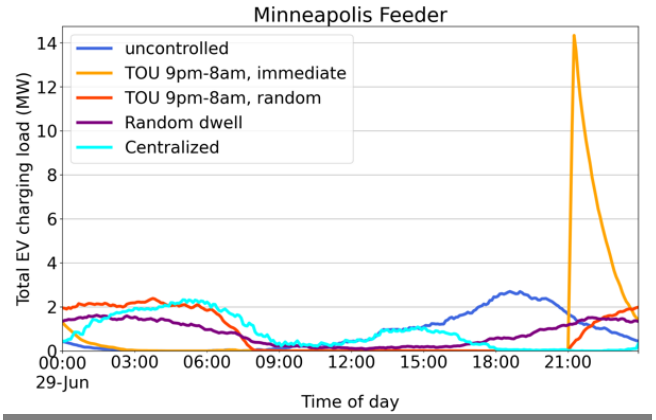

Figure 2. The immediate control highlights a potential timer peak risk in EV load at 9:00 PM. The central control reduces feeder peak and shifts charging to increase load factor, while both of the random controls create a more even distribution.

The average peak line loading increased by 6% in the uncontrolled case, while centralized and random controls only saw a 3% increase. In contrast, immediate control implementation to follow TOU rates could represent as much as a 30% increase. This study shows how proper smart charge controls will help to facilitate the increasing adoption of EVs.

Hydrogen Codes and Standards

2020 U.S. DRIVE Highlight

Hydrogen Wide Area Monitor (HyWAM)

HyWAM's active monitoring capability serves as a research tool to inform facility footprint requirements and enables early detection of unintended releases for improved hydrogen safety.

National Renewable Energy Laboratory

The National Renewable Energy Laboratory's (NREL) Hydrogen Safety Research and Development program has developed a hydrogen wide area monitoring approach (HyWAM) for the temporal and three-dimensional spatial profiling of either intended or unintended hydrogen releases. Active monitoring is recognized as a viable approach to mitigate risks at hydrogen facilities through early detection of unintended hydrogen releases.

As demand has grown, the amount of onsite hydrogen storage has continued to increase at commercial fueling stations. That trend is expected to continue as additional light- and heavy-duty fuel cell electric vehicles are released into the marketplace. As a result, gaseous hydrogen (GH2) storage capacity is frequently proving inadequate and many station developers are opting for on-site liquid hydrogen (LH2), which offers significantly more hydrogen by volume. However, the large setbacks currently required by code preclude the use of LH2 storage at many fueling stations in urban areas. The large LH2 setback is required, in part, because there is a lack of data on the behavior of cryogenic hydrogen releases.

HyWAM can serve as a research tool to empirically profile and elucidate released hydrogen behavior, addressing the current data gap. HyWAM modeling studies and deployment application are interrelated, since the elucidation of released hydrogen behavior can serve to inform HyWAM deployment strategies within an LH2 facility, which in turn could provide risk reduction credits to allow a reduction of setbacks. NREL recently developed a prototype HyWAM system that is based upon a distributed network of hydrogen point sensors integrated with environmental sensors (e.g., wind conditions, temperatures, etc.) and is amenable to commercial deployment. NREL's HyWAM has been used to probe the release behavior of GH2, LH2, and hydrogen-natural gas blends in both indoor and outdoor applications. Recently, a HyWAM system was deployed to profile the behavior of a series of outdoor LH2 releases. The releases were performed under controlled conditions to determine the inter-relationship of release parameters and ambient environmental conditions (e.g., wind conditions and ambient temperature). As shown in Figure 1, an orthogonal wind direction rapidly dissipated the hydrogen plume through turbulent mixing. Alternatively, a steady, in-line wind caused less turbulence, resulting in a broader distribution of hydrogen at higher concentrations. A complete analysis is pending. However, it was shown that HyWAM is a viable method of profiling concentrations of hydrogen from an LH2 release and that these measurements have succeeded in characterizing the impact of wind on cold hydrogen dispersion, which can ultimately inform facility designs.

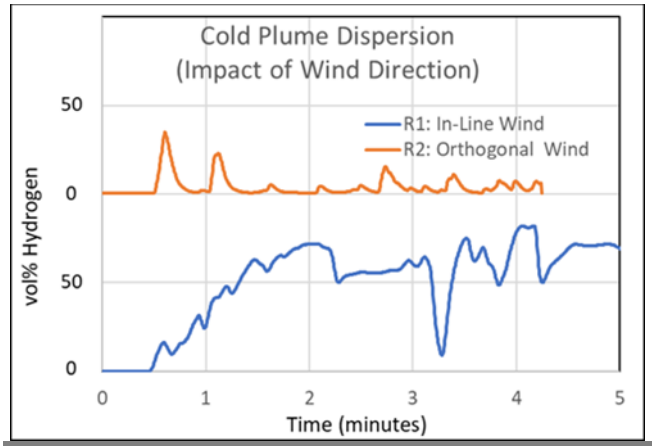

Figure 1. Impact of wind direction for two horizontal LH2 releases (R1 and R2). An orthogonal wind direction facilitates hydrogen dispersion (1 of 32 measurement points are shown for each release).

Hydrogen Delivery and Storage

2020 U.S. DRIVE Highlight

H2FillS: "Hydrogen Filling Simulation" Model to Enable Innovation in Fueling Processes

A publicly available model that simulates gas flow from the hydrogen station to the vehicle storage system, designed to model changes in hydrogen temperature, pressure, and mass flow during filling.

National Renewable Energy Laboratory, Kyushu University, Frontier Energy, and 10 collaborators

A team led by the National Renewable Energy Laboratory (NREL) developed the publicly available software model H2FillS, which can be used to enable changes in hydrogen dispensing methods that lower the cost of fuel. Today, light-duty fuel cell electric vehicles (FCEVs) store approximately 5 kg of hydrogen onboard and are filled in 3-5 minutes using the SAE J2601 fueling protocol. These characteristics require fueling at low temperatures (-40°C) and high pressure (875 bar), necessitating the use of specialized, costly hydrogen fueling station components, thereby making station cost (currently) the largest contributor to the cost of dispensed hydrogen fuel. H2FillS can enable innovations in fueling methods by allowing a user to characterize the impact of changes in fuel temperature on the fill rate and the temperature inside a FCEV's hydrogen tank.

H2FillS is based on a 1-dimensional model that NREL licensed from Kyushu University, validated by using 21 vehicle tank temperature data sets, and expanded with an easy-to-use graphical user interface (GUI) (Figure 1). To validate the model, data sets from experiments conducted previously were obtained from NREL, Honda Motor Company, and PowerTech Labs Inc. Upon validation, the model was shown to predict the temperature and pressure of hydrogen inside an FCEV tank within ± 3.5 K/MPa of experimental results.

NREL is now expanding the H2FillS software to enable 3-dimensional modeling of fueling heavy-duty (HD) FCEVs as part of the Innovating Hydrogen Stations (IHS) project. The model developed under IHS could ultimately inform the development of an HD FCEV fueling protocol. HD FCEVs are expected to store up to 16X more hydrogen onboard than light-duty vehicles and require fueling at rates of over 10 kg/min—5X faster than fueling rates for light-duty FCEVs. Fill protocols for HD FCEVs are currently under development and will be used to inform the design requirements for stations and storage onboard vehicles.

H2FillS was co-funded by the U.S. Department of Energy's Hydrogen and Fuel Cell Technologies Office (HFTO) within the Office of Energy Efficiency and Renewable Energy, along with a large stakeholder base that informed model development, to ensure relevance to industry. Stakeholders included Frontier Energy Inc., Ford Motor Company, General Motors LLC, Honda R&D Americas, Hyundai-Kia America Technical Center, Ivys Energy Solutions Inc., Shell, and Toyota. Additional project partners, collaborators, and technical advisors included staff from Kyushu University, Saga University, Zero Carbon Energy Solutions, Sandia National Laboratories, and Argonne National Laboratory. The IHS project is co-funded by HFTO, Shell, Air Liquide, Toyota, and Honda.

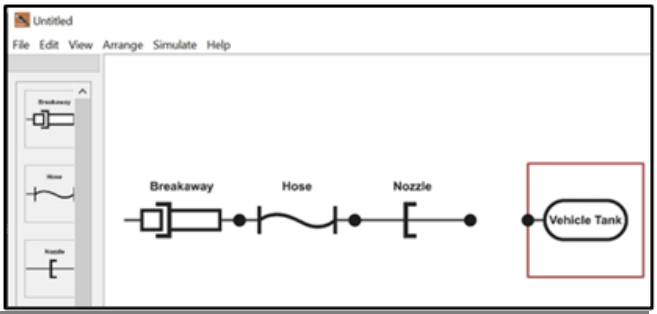

Figure 1. The H2FillS GUI is easy to use to simulate the thermodynamics of hydrogen fueling.

2020 U.S. DRIVE Highlight

50% Carbon Fiber Price Reduction Enabling High Pressure Hydrogen Storage Tanks

Entrepreneurial approach expected to bring carbon fiber cost into the commercially viable range.

University of Virginia, University of Kentucky, Hexagon, Collaborative Composite Solutions Corp., Oak Ridge National Laboratory, and partners

The major impediment to commercially viable high pressure hydrogen tanks is ready to fall. The strength of carbon fiber makes it an excellent technical choice for the overwrapping of 700 bar hydrogen storage tanks, but it has historically been too expensive to use in mass production. Using an entrepreneurial funding mechanism, the U.S. Department of Energy (DOE) is on a path to reduce the cost of carbon fiber (CF) in high pressure storage tanks by 50% over 5 years. This will result in a significant drop in overall storage system cost (Figure 1).

This program uses two innovative methods to attack the goal. Three DOE Energy Efficiency and Renewable Energy Offices (Hydrogen and Fuel Cell Technologies, Vehicle Technologies, and Advanced Manufacturing) are cost sharing this $15 million program. It brings the synergistic expertise and perspective of the multiple Offices to bear on the problem. The program also uses a venture capital-like model of investing in several promising approaches to increase the likelihood of success and down-selecting to a single, most promising project after the first two years of the effort.

The program draws on the full diversity of American innovation. The four projects include teams from both academia (University of Kentucky and University of Virginia) and industry (Hexagon LLC and Collaborative Composite Solutions Corp.). Each team also includes industry and national lab partners. DOE is also funding a parallel effort at Oak Ridge National Laboratory to carry out further research related to carbon fiber cost reduction and testing of fibers produced by the overall effort.

The four projects will adopt different research and development pathways to reduce the cost of carbon fibers and, ultimately, hydrogen storage tanks. Technical strategies the projects will pursue include developing lower cost carbon fiber precursors, developing alternative fiber spinning processes, utilizing advanced fiber conversion techniques, and investigating the use of light-weight, hollow fibers.

In addition to the program's emphasis on reducing carbon fiber cost, each team will also work to improve the overall properties of the carbon fiber composite to further enhance high-pressure tank performance. The final storage tank will at least meet, and is expected to exceed, the performance of existing tanks in critical areas such as gravimetric energy density and burst pressure.

While this program is tightly focused on making carbon fiber for high-pressure hydrogen tanks commercially viable, it is clear that a 50% reduction in carbon fiber cost can also benefit many other areas of American industry where carbon fiber is used.

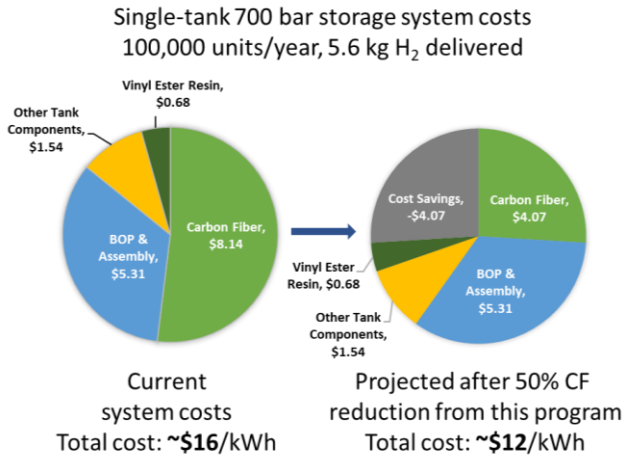

Figure 1. Projected storage system cost reduction via expected 50% reduction in CF costs (and no other cost reductions). Improvement of CF costs will enable an R&D focus in other areas to achieve the long-term storage system targets.

Hydrogen Production

2020 U.S. DRIVE Highlight

Hydrogen from Low- and High-Temperature Electrolysis with Route to $2/kg

New analysis highlights decreasing current and projected hydrogen production costs from low-temperature and high-temperature electrolysis.

Hydrogen and Fuel Cell Technologies Office and Strategic Analysis, Inc

Electrolysis is a commercial process that utilizes electricity to split water to produce hydrogen (H_2). Electrolyzers can be coupled to the electric grid or integrated directly with distributed-generation assets to produce hydrogen for various end uses. To fully understand the state of the industry and to effectively direct R&D funding to critical areas, the Hydrogen and Fuel Cell Technologies Office (HFTO) is actively engaged in working with hydrogen production equipment manufacturers to assess the cost of producing hydrogen. A recent H2A analysis by HFTO shows that **H_2 can be produced via polymer electrolyte membrane (PEM) electrolyzers at a cost of ~$5 to $6/kg-$H_2$**, assuming existing technology, low volume electrolyzer capital costs of $1,500/kW, grid electricity prices ranging from $0.05/kWh to $0.07/kWh, and other H2A standard assumptions.[2] Other published assessments have stated that hydrogen produced via PEM electrolysis can nearly meet the U.S. Department of Energy's (DOE) target of $2/kg and currently ranges from ~$2.50 to $7/kg (Figure 1).

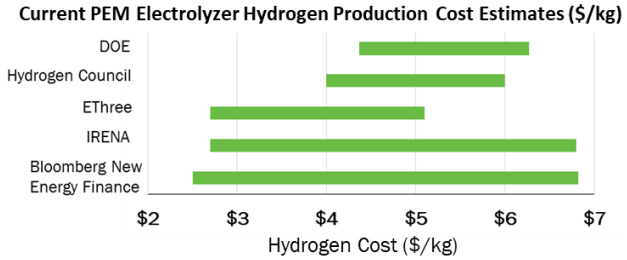

Figure 1. H_2 costs from currently available PEM electrolysis systems from DOE and external stakeholders (2019-2020).

There is also potential to further reduce cost by using high-temperature electrolysis (HTE). This technology can leverage both electricity and heat from generation sources such as nuclear, fossil with CCUS, or concentrated solar power plants to improve conversion efficiencies.

Strategic Analysis Inc. performed a rigorous techno-economic analysis to assess the cost of H_2 produced using HTE in the near- to long-term (Figure 2), assuming electrolyzers are manufactured at scale (700MW/yr) for both current (2019) and projected future (2035) technology years. The resulting H2A projected untaxed **H_2 cost was shown to range from approximately $2 to $6/kg H_2** using industry input on HTE system performance as well as capital, operational, and feedstock costs.[3] When these systems are coupled to low-cost electricity, in line with recent developments of renewable energy, the cost of producing hydrogen is reduced to the $2/kg target.

Realizing these cost projections will require continued R&D to improve electrolyzer durability and manufacturability. Consistent and widely available low-cost and low-carbon electricity is also key to enabling low-cost, sustainable H_2 production.

Central H_2 HTE	Low ($/kg H_2)	Baseline ($/kg H_2)	High ($/kg H_2)	3¢/kWh ($/kg H_2)
Projected Current	$2.50	**$4.16**	$5.71	$2.36
Projected Future	$2.27	**$3.89**	$5.43	$2.00

Figure 2. H_2 Production High-Volume HTE Cost Projections.

[2] https://www.hydrogen.energy.gov/pdfs/20004-cost-electrolytic-hydrogen-production.pdf.

[3] https://www.hydrogen.energy.gov/pdfs/20006-production-cost-high-temperature-electrolysis.pdf.

2020 U.S. DRIVE Highlight

Advancements in Photoelectrochemical Hydrogen Production Enabled by HydroGEN Consortium

Durability and efficiencies improved simultaneously through highly successful collaborations.

Rutgers University and University of Michigan, in Collaboration with HydroGEN

Photoelectrochemical (PEC) devices have the potential to enable sustainable, low-cost hydrogen (H_2) by directly using sunlight to split water, bypassing the need for (and cost of) electricity. Combining semiconductor photoelectrodes and photocatalysts, PEC systems are still in an early stage of development. As such, the PEC field has benefited considerably as a focus area of the HydroGEN Consortium. HydroGEN was initiated in 2016 and broadly aims to accelerate materials R&D for advanced water splitting pathways through streamlined access to our National Laboratories' world class capabilities and expertise. Specifically for PEC, HydroGEN efforts have yielded improvements in device efficiency and durability. In order to realize a hydrogen cost goal of $2/kg, PEC devices will need high solar-to-hydrogen (STH) efficiencies (potentially more than 20% depending on material cost) and an electrode durability on the order of years. Current PEC state of the art can either obtain high efficiency or long durability, but not both at the same time. These collaborations made significant progress in meeting both goals simultaneously.

During the first phase of HydroGEN, Rutgers University collaborated with the National Renewable Energy Laboratory (NREL) to create high-performance PEC devices without the use of noble metal catalysts. The team demonstrated how to stabilize a tandem photoabsorber against corrosion while maintaining its optical performance. This was accomplished by depositing a platinum group metal (PGM)-free hydrogen evolution reaction (HER) catalyst on a substrate made of ultrathin anti-reflective and diffusion barrier layers. The Rutgers and NREL teams optimized the optical absorption and electrical properties of the materials and interfaces. The resulting PEC device exhibits stable operation for 200 hours and STH efficiencies of 11%-13%, with no applied bias at neutral pH in phosphate electrolyte (Figure 1 A). This is well over an order of magnitude improvement in durability for a base metal junction.

Another successful PEC HydroGEN collaboration involving the University of Michigan with NREL, and Lawrence Berkeley and Lawrence Livermore National Laboratories achieved a STH efficiency of 10% for over 3,000 hr operation using a Ga(In)N/Si double-junction photocathode. This device was observed to have a novel self-healing behavior. Advanced computational methods identified the formation of a stabilizing, ultrathin gallium oxynitride layer (Fig. 1B) and provided fundamental insights on how this phenomenon aided the performance. This layer also displays a higher density of catalytic sites for HER, which opens a promising opportunity to minimize PGM catalysts.

The highly collaborative work within HydroGEN is addressing fundamental stability/photocorrosion barriers of PEC H_2 production. With continued improvements in durability and efficiency, large-scale PEC systems for sustainable, low-cost H_2 production are becoming more promising.

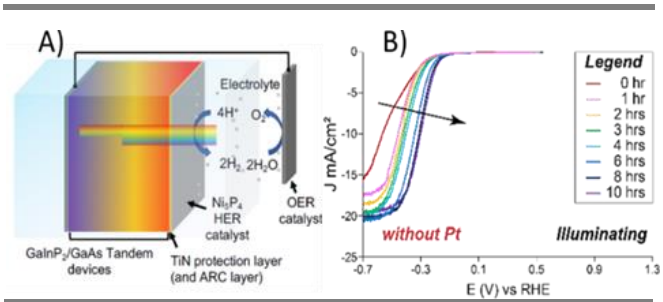

Figure 1. A) Schematic of Rutgers' PEC device that simultaneously achieved STH >12% and > 200h durability. B) Improved PEC performance with increasing illumination time for U. Michigan device through formation of oxynitride layer

Net-Zero Carbon Fuels

2020 U.S. DRIVE Highlight

Assessment of Multiple Pathways for Producing Carbon-Neutral Fuels

Understanding the carbon intensity implications of several fuel pathways optimized to minimize GHG production through complimentary life-cycle assessments and technoeconomic analyses.

Argonne National Laboratory, Lawrence Livermore National Laboratory, National Renewable Energy Laboratory, and Pacific Northwest National Laboratory

Researchers at the national laboratories evaluated several pathways for their potential to produce "net-zero carbon" fuels. The required technologies were optimized for reducing carbon intensity (CI) and researchers assessed the techno-economics of these pathways to understand the associated cost of carbon mitigation for a given process. Researchers investigated several advanced carbon management strategies for their potential to lower the CI of fuels and to understand their implementation costs. The team considered conventional biofuel inputs such as corn starch, as well as lignocellulosic biomass, algae and carbon dioxide (CO_2). Researchers selected four unique fuel pathways for scrutiny to discern their costs and benefits and their ability to provide net-zero carbon fuels. Select results from two pathways are discussed here to illustrate the key accomplishments from 2020. In-depth analyses of all four pathways can be found in the pending *FY20 Net-Zero Tech Team Analysis Summary Report*.

One pathway examined converting corn starch to ethanol, with carbon capture and sequestration (CCS) in place on the fermentation. This pathway has a CI ranging from 15 (CCS-only) down to -9 gCO_2/MJ when using renewable electricity and renewable natural gas (RNG) as process inputs, as well as utilizing fertilizer made from low-carbon inputs. These values are significantly lower than the 91 gCO_2/MJ of petroleum-derived gasoline (see Figure 1). The selling price of this fuel ranged from \$1.92 with CCS-only to \$2.33/gal-ethanol in the expanded pathway (approximately \$2.95–\$3.50/gal-gasoline equivalent [GGE]).

Another pathway examined ethanol production via syngas fermentation, with the syngas coming from either woody biomass gasification or from CO_2 electrocatalysis, which could leverage an increasing renewable electricity system. This pathway has a CI ranging from well over 4 times of that of the fossil fuel baseline when 2018 grid mix electricity is used to convert CO_2, to 16.8 gCO_2/MJ under a base case biomass gasification approach, to 5.1 gCO_2/MJ when entirely renewable electricity is used to convert CO_2. Fuel price is estimated at \$1.60/gal-ethanol (\$2.46/GGE) for biomass gasification, \$6.55/gal-ethanol (\$9.96/GGE) for CO_2 electrocatalysis with a 2018 grid mix at 7¢/kWh, and \$3.21/gal-ethanol (\$4.87/GGE) in a future renewable grid scenario at 2¢/kWh.

Both select pathways offer insight into the challenges and opportunities for generating net-zero fuels and meeting the growing interest. The Net-Zero Technical Team will explore these technologies and others in the coming year.

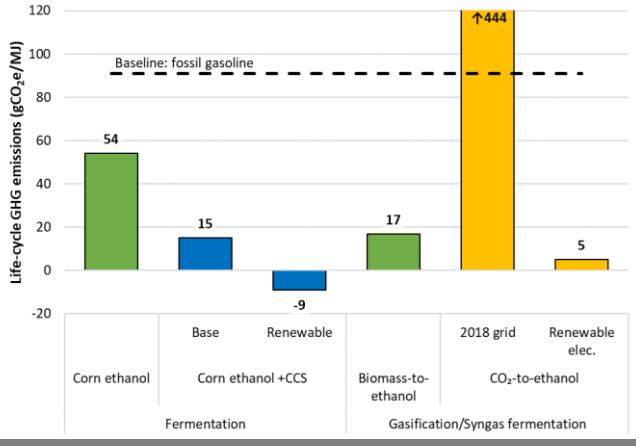

Figure 1. Life-cycle greenhouse gas emissions associated with generating ethanol from three different resources.

Vehicle and Mobility Systems Analysis

2020 U.S. DRIVE Highlight

VMSATT Future Mobility Scenario Development

Defining near-term and long-term technology, infrastructure and policy combinations to assess their impact on a mobility system.

Vehicle and Mobility Systems Analysis Tech Team

A mobility system is the collection of all the interacting elements (all modes of travel, users, infrastructure) in a specific travel setting (e.g., Chicago metro area). VMSATT is tasked with assessing the impact of vehicle and V2X technologies (e.g., adaptive cruise control, vehicle-to-vehicle and vehicle-to-infrastructure communications), as well as policy and infrastructure impacting vehicle usage, on the mobility system in which they are deployed.

VMSATT's diverse group of vehicle and transportation system experts to develop an initial series of scenarios detailing deployment of selected vehicle technology, infrastructure and travel policy options to assess their impact on vehicle energy consumption, travel time and other relevant measures in the context of a mobility system.

- The scenarios define low and high option penetration in the near-future (2025), and longer term (2035)
- Initial Vehicle technology options selected are: Adaptive Cruise Control, Connected Adaptive Cruise Control, En-Route ECO-navigation and Driving Advisory Interfaces (V2I)
- Initial smart infrastructure options selected are: Variable Speed Limit Advisory, Intersection Flow Control, and Coordinated On-Ramp Merging
- Initial policy and planning options are: Low/Zero-Emission Zones, Bus Lanes, HOV/Ride-Sharing/EV Lane, and Connected Autonomous Vehicle Corridors

The options described above can be combined in any desired combination to assess their impact on the overall mobility system and the vehicles operating in it. The first scenario to be analyzed will be the separate and combined impacts of adaptive and connected adaptive cruise control on vehicle operation in the Chicago metropolitan area. Limiting the initial set of options will allow us to test the practicality of assessing the sensitivity of individual options on the mobility system. The analysis will also serve as a test case for fine-tuning the development and selection of inputs for other mobility scenarios.

The mobility system analysis utilizes the Systems and Modeling for Accelerated Research in Transportation (SMART) workflow (see figure) developed by the DOE Vehicle Technology Office. The analysis will be executed by the System Modeling group at Argonne National Labs.

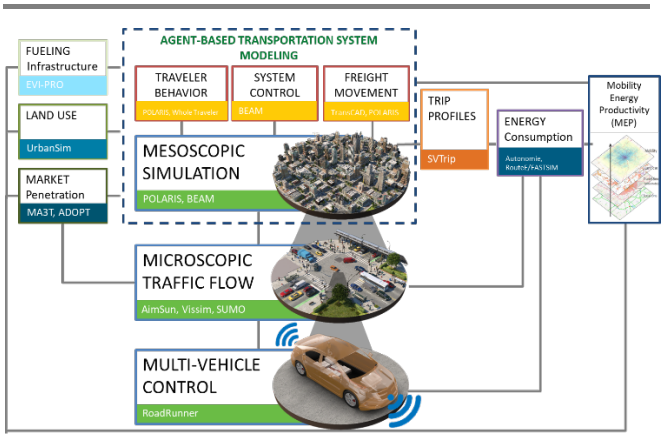

Figure 1. DOE VTO Energy Efficient Mobility Systems SMART Workflow

(This Page Intentionally Left Blank)